LAWRENCE
LIVERMORE
NATIONAL
LABORATORY

LLNL-TR-801481

MULTICHANNEL SPECTRAL ESTIMATION: An Approach to Estimating/Analyzing Vibrational Systems

J. V. Candy

January 15, 2020

Disclaimer

This work performed under the auspices of the U.S. Department of Energy by Lawrence Livermore National Laboratory under Contract DE-AC52-07NA27344.

MULTICHANNEL SPECTRAL ESTIMATION: An Approach to Estimating/Analyzing Vibrational Systems

J. V. Candy

Dynamic structures either operational or under test require complex spectral analysis in order to characterize their modal responses. In some applications constant vigilance in terms of analysis or potential failures demand an accurate methodology to estimate both modal frequencies as well as mode shapes. Multichannel versus single channel processing can create a dilemma especially when specific modes are *not* excited across all measurement channels or weakly excited implying multichannel techniques are required to extract them from noisy data. Here we investigate a suite of both classical and modern parametric spectral estimation techniques to extract modal frequencies based on synthesized multiple input/multiple output (MIMO) structural data.

1 INTRODUCTION

Structural systems operating in noisy environments create a challenging analysis and monitoring problem in order to estimate their signatures in real-time and predict potential anomalies that can lead to catastrophic failure. In order to estimate the condition of a structure from noisy vibration measurements, it is necessary to identify features that make it unique such as emitted resonant (modal) frequencies that offer a signature characterizing its condition. The monitoring of structural modes to estimate the condition of a device under investigation is essential, especially if it is a critical entity of an operational system. Many simple algorithms like the fast-Fourier transform coupled with spectral peak-picking offer a technique to extract modal frequencies of a structural object for both computational speed and accuracy [1]-[7]. Here we investigate a suite of multichannel spectral estimation techniques that enables an accurate extraction of modal frequencies from noisy uncertain measurements.

Spectral estimation is a necessary methodology to analyze the frequency content of noisy data sets. Many techniques have evolved starting with the classical Fourier transform methods based on the well-known Wiener-Khintchine relationship relating the covariance-to-spectral density as a transform pair culminating with more elegant model-based, parametric techniques that apply prior knowledge of the data to produce a high-resolution spectral estimate [8], [9]. The popular *correlation* or so-called *Blackman-Tukey* method [9] that Fourier transforms a windowed covariance satisfying the Wiener-Khintchine relationship directly was developed with the advent of the fast Fourier transform (*FFT*). Currently for long data records, the most popular approach is the Welch Periodogram Method (*WPM*) that is based on averaging normalized periodograms estimated from windowed, overlapped sections of data

[1]. Here the usual trade-off between estimator *bias/variance* dominates the spectral design.

Multichannel spectral representations of structural systems are a class of both parametric as well as non-parametric estimators that provide improved spectral estimates especially for vibrating mechanical structures. Excitations of these structures can be problematic, since some of the underlying modes may be weakly excited or not excited at all depending on the type and locations of the input signal. In any case, the classical multichannel Blackman-Tukey (*BTM*) and Welch (*WPM*) techniques can provide reasonable estimates when coupled with modal "peak-peaking" methods as long as the signal-to-noise ratio (*SNR*) is reasonably high. Parametric multichannel methods can perform quite well in low *SNR* environments even when applying simple peak-picking techniques. In this report we investigate the performance of both nonparametric and parametric multichannel spectral estimation methods when applied to synthesized noisy, structural vibration data.

The classical non-parametric *BTM* and *WPM* are applied to the data set, first, followed by the parametric approaches consisting of the Yule-Walker (*YWM*), Burg-lattice (*BLMorfV*, *BLNutS*), Minimum Variance (*MVM*) methods all employing the multichannel autoregressive (*AR*) all-pole model. Next the model-based methods (*MBM*) follow based on the linear, time invariant (*LTI*) multichannel state-space (*SSP*) representation of the vibrating structure consisting on an embedded mass-damper-spring (*MCK*) model. All of these methods are analyzed output channel-by-output channel, since some modes are not strongly excited (low *SNR*) and are not spectrally visible in a given channel.

In Sec. 2, we first define the multichannel spectral estimation problem and then proceed to briefly develop both the corresponding *AR* and *SSP*-model sets used throughout. Multichannel spectral estimation techniques are developed in Sec. 3 starting with the classical, Blackman-Tukey (correlation) method (*BTM*) and Welch Periodogram method (*WPM*) followed by the Yule-Walker (*YWM*), Burg-lattice, Morf-Viera (*BLMorfV*), Nutall-Strand (*BLNutS*), and the minimum variance method (*MVM*) evolving to the model-based FULL (stochastic realization) and FAST (constrained) state-space approaches. In Sec. 4, vibrational systems are developed for both single channel as well as multichannel *MCK*-systems leading to the state-space representations. The synthesis of noisy acceleration measurements for a multichannel structure is discussed in Sec. 5 and used as test data for the various methods. Performance analysis of these algorithms is discussed for comparative purposes with the results of this effort summarized in the final section.

2 Multichannel Models

In this section we develop multiple channel (output) models starting with a set of input/output representations eventually leading to more physics-based representations based on state-space models. Typical deterministic multiple input/multiple output (*MIMO*) sys-

tems can be characterized by their impulse response matrices or equivalently multichannel transfer function matrices given by

$$\mathbf{y}(t) = \mathcal{H}(t) \star \mathbf{u}(t) = \int_{\tau=0}^{t} \mathcal{H}(t-\tau)\mathbf{u}(\tau)d\tau \tag{1}$$

for $\mathbf{y} \in \mathrm{R}^{N_y \times 1}$ the vector of outputs or measurements, $\mathbf{u} \in \mathrm{R}^{N_u \times 1}$ the vector of inputs or excitations, $\mathcal{H} \in \mathrm{R}^{N_y \times N_u}$ the *impulse response matrix* and $\star$ the multichannel *convolution* operator where

$$\mathcal{H}(t) = \begin{bmatrix} h_{11}(t) & \cdots & h_{1N_u}(t) \\ \vdots & \ddots & \vdots \\ h_{N_y1}(t) & \cdots & h_{N_yN_u}(t) \end{bmatrix} \tag{2}$$

Equivalently, taking the Laplace transform of Eq. 1, ($\mathbf{Y}(s) = \mathcal{L}(y(t))$), we obtain the frequency domain representation ($s = \sigma + j\omega$)

$$\mathbf{Y}(s) = \mathcal{H}(s) \times \mathbf{U}(s) \tag{3}$$

with the $N_y \times N_u$ *transfer function matrix* defined by the ratio of outputs-to-inputs for

$$\mathcal{H}(s) = \frac{\mathbf{Y}(s)}{\mathbf{U}(s)} = \begin{bmatrix} H_{11}(s) & \cdots & H_{1N_u}(s) \\ \vdots & \ddots & \vdots \\ H_{N_y1}(s) & \cdots & H_{N_yN_u}(s) \end{bmatrix} \tag{4}$$

Rather than a vector of deterministic inputs, $\{\mathbf{u}\}$, suppose it is *random*, then we can replace the deterministic relationship in terms of their stochastic counterparts—the correlation and power spectra assuming a zero-mean, stationary processes. That is, the multichannel *correlation matrix* defined by $\mathcal{R}_{ij} := E\{y(i)(t)u(t+\tau\}$

$$\mathcal{R}_{yu}(\tau) = \begin{bmatrix} R_{11}(\tau) & \cdots & R_{1N_u}(\tau) \\ \vdots & \ddots & \vdots \\ R_{N_y1}(\tau) & \cdots & R_{N_yN_u}(\tau) \end{bmatrix} \tag{5}$$

Again taking the Laplace transform of the correlation matrix ($\mathbf{S}(s) = \mathcal{L}(\mathcal{R}_{yu}(\tau))$, we obtain the frequency domain representation (Wiener-Khintchine relation [9]) or the *multichannel power spectrum matrix* given by [18])

$$\mathcal{S}_{yu}(s) = \begin{bmatrix} S_{11}(s) & \cdots & S_{1N_u}(s) \\ \vdots & \ddots & \vdots \\ S_{N_y1}(s) & \cdots & S_{N_yN_u}(s) \end{bmatrix} \tag{6}$$

for $S_{ij}(s) := \mathcal{L}\{R_{ij}(\tau)\}$.

Continuous-time processes provide the insight into the overall operational aspects of system performance but with "fast" digitizers coupled to on-board sensors, it makes more

sense to consider their sampled-data/discrete counterparts. With this in mind, sampled-data systems evolve quite easily, that is, replacing time with sampled time $t \rightarrow t_k$, we have that the impulse response of continuous-time leads to

$$\mathbf{y}(t_k) = \mathcal{H}(t_k) \star \mathbf{u}(t_k) = \sum_{k=0}^{K} \mathcal{H}(t_k - \tau_k)\mathbf{u}(\tau_k) \tag{7}$$

All of the relations (above) follow as well for $t \rightarrow t_k$ with the discrete-time *Z-transform* ($\mathcal{Z}$) replacing the continuous-time Laplace transform ($\mathcal{L}$) leading to the sampled/discrete transfer function, $\mathcal{H}(s) \rightarrow \mathcal{H}(z)$[1]) such that

$$\mathbf{Y}(z) = \mathcal{H}(z) \times \mathbf{U}(z) \tag{8}$$

with the *sampled* or *discrete-time* $N_y \times N_u$ transfer function matrix, $\mathcal{H}(z)$ defined by the ratio of outputs-to-inputs as before.

Discrete random vector inputs $\mathbf{u}(t_k)$ also lead to a version of the Wiener-Khintchine relation for the discrete-time case as

$$S_{yu}(z) := \mathcal{Z}\{R_{yu}(\ell)\} \tag{9}$$

Therefore, the *multichannel spectral estimation problem* is simply:

GIVEN a set of N_u-input sequences and N_y output sequences, FIND an estimate of the corresponding $N_y \times N_u$-power spectrum matrix, $\mathcal{S}_{yu}(z)$

With this background and definitions in mind, we can now proceed to investigate various multichannel discrete-time relations that will lead to a suite of spectral estimators.

2.1 Multichannel Models: Input/Output (Autoregressive Moving Average Representation)

The multichannel input/output or equivalently *autoregressive moving average* ($ARMA$) model is defined by the matrix polynomials

$$\mathbf{y}(t) = -\sum_{k=1}^{N_a} \mathcal{A}_k \mathbf{y}(t-k) + \sum_{k=0}^{N_b} \mathcal{B}_k \mathbf{u}(t-k) \tag{10}$$

where $\mathcal{A}_k \in \mathcal{R}^{N_y \times N_y}$ and $\mathcal{B}_k \in \mathcal{R}^{N_y \times N_u}$ are the sets of matrix polynomials.

[1]The $\mathcal{Z}$-transform is the discrete-time equivalent of the Laplace transform of continuous-time and is related through the impulse invariant transformation given by $\mathcal{Z} = e^{s\triangle T}$.

Taking the $\mathcal{Z}$-transform of Eq. 10 gives the input/output relationship in the frequency domain as

$$\mathbf{Y}(z) = \underbrace{\mathcal{A}^{-1}(z)\mathcal{B}(z)}_{\mathcal{H}(z)}\mathbf{U}(z) \tag{11}$$

for $\mathcal{A}(z) = \mathbf{I} + \sum_{k=1}^{N_a} A_k z^{-k}$ and $\mathcal{B}(z) = \mathbf{I} + \sum_{k=1}^{N_b} B_k z^{-k}$.

The corresponding discrete transfer function in terms of the matrix polynomials is given by

$$\mathcal{H}(z) = \frac{\mathbf{Y}(z)}{\mathbf{U}(z)} = \mathcal{A}^{-1}(z)\mathcal{B}(z) \tag{12}$$

for $\mathcal{H}(z) \in \mathcal{R}^{N_y \times N_u}$.

As before, in terms of matrix polynomials for random vector signals, we have the multichannel power spectrum defined by

$$\mathcal{P}_{yy}(z) = \mathcal{H}(z) \times \mathcal{H}^{\dagger}(z) = \left(\mathcal{A}^{-1}(z)\mathcal{B}(z)\right) \times \mathcal{P}_{uu}(z) \times \left(\mathcal{A}^{-1}(z^*)\mathcal{B}(z^*)\right)^{\dagger} \tag{13}$$

where $*$ is the complex conjugate and † is the Hermitian conjugate operation.

For spectral estimation purposes, we will simplify the *ARMA*-model to an *all-pole* or equivalently *autoregressive* (*AR*) representation such that $(\mathbf{u} \rightarrow \mathbf{e}, \mathcal{B} \rightarrow I)$, that is, Eq. 10 becomes

$$\mathbf{y}(t) = -\sum_{k=1}^{N_a} \mathcal{A}_k \mathbf{y}(t-k) + \mathbf{e}(t) \tag{14}$$

where $\mathbf{e}$ is a random, zero-mean, white noise vector with corresponding variance matrix R_{ee}.

For this case the power spectrum simplifies to

$$\mathcal{P}_{yy}(z) = \mathcal{H}(z) \times \mathcal{H}^{\dagger}(z) = \mathcal{A}^{-1}(z) \times R_{ee} \times \left(\mathcal{A}^{-1}(z^*)\right)^{\dagger} \tag{15}$$

The stationary N_a-channel autoregressive process can be also be expressed as a block vector product

$$\mathbf{e}_{N_a}(t) = \mathbf{a}_{N_a} \times \mathbf{y}_{N_a}(t) \tag{16}$$

where

$$\mathbf{a}_{N_a} = \begin{bmatrix} \mathbf{I}_{N_a} & \mathbf{A}_{N_a}(1) \cdots \mathbf{A}_{N_a}(N_a) \end{bmatrix}$$

and $\mathbf{y}_{N_a} \in \mathcal{R}^{N_a} \times 1$.

2.2 Multichannel Models: State-Space Representation

State-space representations have become an integral component of mechanical systems especially in the area of health monitoring. Since we sample the continuous-time system, we will employ a discrete state-space representation and then transform the results back to the continuous-time domain, when required, for eventual modal analysis.

The generic linear, time invariant, deterministic, *state-space* model is defined by its system matrix A, input transmission matrix B and output (measurement) matrix C for *discrete-time* systems as

$$\begin{aligned} \mathbf{x}(t+1) &= A\mathbf{x}(t) + B\mathbf{u}(t) && \text{[State]} \\ \mathbf{y}(t) &= C\mathbf{x}(t) && \text{[Output]} \end{aligned} \tag{17}$$

for the state $\mathbf{x} \in R^{N_x \times 1}$, input $\mathbf{u} \in R^{N_u \times 1}$, and output $\mathbf{y} \in R^{N_y \times 1}$.

Corresponding to this representation is the discrete *transfer function* in terms of the $\mathcal{Z}$-transform

$$\mathcal{H}(z) = C(zI - A)^{-1}B \tag{18}$$

with the corresponding *impulse response* termed the Markov parameters [10], [11]

$$\mathcal{H}(t) = CA^{t-1}B \tag{19}$$

Expanding the state equations, it is easily shown that [11]

$$\mathbf{x}(t) = A^t\mathbf{x}(0) + \sum_{k=0}^{t-1} A^{t-k-1}B\mathbf{u}(k-1); \qquad t = 0, 1, \cdots, K \tag{20}$$

and therefore the output is given by

$$\mathbf{y}(t) = CA^t\mathbf{x}(0) + \sum_{k=0}^{t-1} CA^{t-k-1}B\mathbf{u}(k-1) \tag{21}$$

With the state-space representation in mind and assuming again that $\mathbf{u}$ is zero-mean, random white noise, we can easily cast the multichannel spectral estimation problem into this framework. Recall that the output power spectrum[2] is given by

$$\mathcal{P}_{yy}(z) = \mathcal{H}(z) \times \mathcal{H}^{\dagger}(z) = \left(C(zI - A)^{-1}B\right) \times R_{uu} \times \left(C(z^*I - A)^{-1}B\right)^{\dagger} \tag{22}$$

Therefore, we see that both the multichannel autoregressive and state-space models can be used to: (1) represent multichannel systems; and (2) parameterize the multichannel

[2]We have ignored measurement noise for simplicity.

power spectrum that can be used to solve our underlying modal problem to follow. This completes the set of multichannel models that we will exploit in this report, next we consider the mechanical systems that we investigate throughout.

3 Multichannel Spectral Estimation

With the initial application of Fourier analysis techniques to raw sun-spot data over 200 years ago, the seeds of spectral estimation were sown by Schuster [12]. Fourier analysis for random signals evolved rapidly after the discovery of the Wiener-Khintchine theorem relating the covariance and power spectrum. Finally with the evolution of the fast Fourier transform (see Cooley [8]) and digital computers, all of the essential ingredients were present to establish the classical approach to classical or nonparametric spectral estimation.

Spectral estimation techniques have been developed and improved over the years with one major task in mind—the analysis of random data. A majority of the initial effort was focused on applying the Wiener-Khintchine theorem and transform theory, while modern parametric techniques evolved primarily from the "speech" community [13], [14]. In this section, we discuss popular classical (nonparametric) methods that are viable, when *long* data records are available. We make no attempt to provide detailed derivations of the algorithms that are available in other texts [13], [15], [16], [17], but just follow a brief outline of the approach and present the final applicaton results.

Classical spectral estimators typically fall into two categories: direct and indirect. The direct methods operate directly on the raw data to transform it to the frequency domain and produce the estimate. Indirect methods, first estimate the covariance sequence and then transform to the frequency domain–an application of the Wiener-Khintchine theorem. We discuss two basic nonparametric multichannel spectral estimation techniques: the correlation method (indirect) and the periodogram method (direct).

3.1 Classical Non-Parametric Multichannel Correlation or Blackman-Tukey Method (BTM)

The *correlation method* or sometimes called the Blackman-Tukey method (BTM) is simply an implementation of the Wiener-Khintchine theorem: the covariance is obtained using a sample covariance estimator and then the power spectral density (PSD) is estimated by calculating the *discrete Fourier transform* (DFT). The DFT transform pair is defined by

$$\mathbf{Y}(\Omega_m) \;:=\; DFT\Big[\mathbf{y}(t)\Big] = \sum_{t=0}^{M-1} \mathbf{y}(t) e^{-j\Omega_m t}$$

$$\mathbf{y}(t) \quad = \quad IDtFT\Big[\mathbf{Y}(\Omega_m)\Big] = \frac{1}{M}\sum_{t=0}^{M-1}\mathbf{Y}(\Omega_m)e^{j\Omega_m t} \tag{23}$$

for $\Omega_m = \frac{2\pi}{M}m$ where it can be thought of as the *DtFT* with $\Omega \to \Omega_m$, that is, the *DtFT* sampled uniformly around the unit circle [15].

The multichannel case with $y \to \mathbf{y}$ and $Y \to \mathbf{Y}$ leads to the multichannel correlation/spectrum matrices with sample correlation estimate

$$\hat{\mathbf{R}}_{yy}(\ell) = \frac{1}{K}\sum_{t=1}^{K-|\ell|}\mathbf{y}(t+\ell)\mathbf{y}^{\dagger}(t) \tag{24}$$

and the corresponding correlation matrix is

$$\mathcal{R}_{yy}(\tau) = \begin{bmatrix} \hat{\mathbf{R}}_{yy}(0) & \cdots & \hat{\mathbf{R}}_{yy}(K) \\ \vdots & \ddots & \vdots \\ \hat{\mathbf{R}}_{yy}(-K) & \cdots & \hat{\mathbf{R}}_{yy}(0) \end{bmatrix} \tag{25}$$

Again taking the Fourier transform of the correlation matrix ($\mathcal{S}(\Omega_m) = \mathrm{DtFT}(\mathrm{R}_{yy}(\ell))$, we obtain the frequency domain representation (Wiener-Khintchine relation [9]) or the *multichannel power spectrum matrix*, that is, [18]

$$\hat{\mathbf{S}}_{yy}(\Omega) = \frac{1}{M}\sum_{t=1}^{M}\hat{\mathbf{R}}_{yy}(\ell)e^{-j\Omega_m t} \tag{26}$$

given by

$$\mathcal{S}_{yy}(\Omega) = \begin{bmatrix} \hat{\mathbf{S}}_{yy}(1,1) & \cdots & \hat{\mathbf{S}}_{yy}(1,M) \\ \vdots & \ddots & \vdots \\ \hat{\mathbf{S}}_{yy}(M,1) & \cdots & \hat{\mathbf{S}}_{yy}(M,M) \end{bmatrix} \tag{27}$$

for $S_{yy}(i,j) := \mathcal{L}\{R_{ij}(\ell)\}$.

Therefore, we have that

$$\hat{\mathcal{S}}_{yy}(\Omega) \quad = \quad \mathrm{DtFT}\Big[\hat{\mathcal{R}}_{yy}(\ell)\Big]$$

$$\hat{\mathcal{R}}_{yy}(\ell) \quad = \quad \mathrm{IDtFT}\Big[\hat{\mathcal{S}}_{yy}(\Omega)\Big]$$

This transform approach tends to produce a noisy spectral estimate; however, a smoothed estimate can be obtained by multiplying each R_{yy} by a *window function*, $\mathcal{W}$ usually called a *lag window*. The window primarily reduces spectral leakage and improves the estimate. It is also interesting to note that a sample covariance estimator does not guarantee the positivity of the *PSD* (auto) when estimated directly from the Wiener-Khintchine theorem

[15]. However, if the estimator is implemented directly in the Fourier domain, then it will preserve this property, since it is the *square* of the Fourier spectrum.

We summarize the *correlation method* (Blackman-Tukey) of spectral estimation by:[3]

Correlation (Blackman-Tukey) Method (*BTM*) Spectral Estimation:

1. *Calculate* the *DFT* of $\mathbf{y}(t)$, that is, $\mathbf{Y}(\Omega_m)$
2. *Multiply* $\mathbf{Y}(\Omega_m)$ by its Hermitian conjugate to obtain, $\mathbf{Y}(\Omega_m) \times \mathbf{Y}^\dagger(\Omega_m)$
3. *Estimate* the covariance from the *IDFT*, $\hat{\mathbf{R}}_{yy}(k) = IDFT\Big[|\mathbf{Y}(\Omega_m)|^2\Big]$
4. *Multiply* the covariance by the lag window $\mathcal{W}(k)$, and
5. *Estimate* the *PSD* from the *DFT* of the windowed covariance, $\hat{S}_{yy}(\Omega_m) = DFT\Big[\hat{\mathbf{R}}_{yy}(\ell) \times \mathcal{W}(k)\Big]$

These correlation spectral estimates are statistically improved by using a lag or equivalently spectral window.[4] With practical window selection and long data records, the correlation method can be effectively utilized to estimate the *PSD* (see [15] for more details).

3.2 Classical Non-Parametric Welch Average Periodogram Method (*WPM*)

Next we consider a more direct approach to estimate the *PSD*. We introduce the concept of a periodogram estimator with statistical properties equivalent to the correlation method, then we show how to improve these estimates by statistical averaging and window smoothing leading to *Welch's method* of spectral estimation, that is, the Welch Periodogram Method (*WPM*) [1]. The periodogram was devised by statisticians to detect periodicities in noisy data records [12]. The improved method of spectral estimation based on the so-called *periodogram* defined by

$$\mathbf{P}_{yy}(\Omega_m) := \frac{1}{M}\Big(\mathbf{Y}(\Omega_m) \times \mathbf{Y}^\dagger(\Omega_m)\Big) = \frac{1}{M}\Big|\mathbf{Y}(\Omega_m)\Big|^2$$

The samples of $\mathbf{P}_{yy}$ are uncorrelated, suggesting that one way of reducing the variance in $\mathbf{P}_{yy}$ is to *average* individual periodograms obtained by *sectioning* the original N point data record into K, L-point sections, that is,

[3]Note also if we replace X^* by Y^* we can estimate the cross correlation $\hat{R}_{xy}(k)$ and corresponding cross spectrum $\hat{S}_{xy}(\Omega_m)$ using this method.

[4]The window function is called a *lag window* in the time or lag domain $\mathcal{W}(k)$ and a *spectral window* in the frequency domain $\mathcal{W}(\Omega_m)$ with its maximum at the origin to match that property of the autocorrelation function; therefore, it is sometimes called a "half" window.

$$\hat{\mathbf{S}}_{yy}(\Omega_m) = \frac{1}{K}\sum_{i=1}^{K}\hat{\mathbf{P}}_{yy}(\Omega_m, i)$$

where $\hat{\mathbf{P}}_{yy}(\Omega_m, i)$ is the i-th, L-point periodogram. If x is stationary, then it can be shown that this estimate is consistent, since the variance approaches zero as the number of sections become infinite [15]. For the periodogram estimator, we have

$$var \propto \frac{1}{K} \quad \text{and} \quad bias \propto \frac{K}{N}$$

So we see that for K large, the variance is inversely proportional to K, while the bias is directly proportional. Therefore for a *fixed* record length N as the number of periodograms increases, variance decreases, but the bias increases. This is the basic tradeoff between variance and resolution (bias) which can be used to determine a priori the required record length $N = LK$ for an acceptable variance. A *full* window, $\mathcal{W}(t)$, can also be applied to obtain a smoothed spectral estimate.

Welch [1] introduced a modification of the original procedure. The data is sectioned into K records of length L; however, the window is applied directly to the segmented records *before* periodogram computation. The modified periodograms are then

$$\hat{\mathbf{P}}(\Omega_m, i) = \frac{1}{U}\left|DFT\Big[\mathbf{y}_i(t)\mathcal{W}(t)\Big]\right|^2 \quad i = 1, \ldots, K$$

where

$$U = \frac{1}{L}\sum_{t=0}^{L-1}\mathcal{W}^2(t)$$

and

$$\hat{\mathbf{S}}_{yy}(\Omega_m) = \frac{1}{K}\sum_{i=1}^{K}\hat{\mathbf{P}}(\Omega_m, i)$$

We summarize the *average periodogram method* (Welch's procedure) by:

Average Periodogram (Welch) Method (*WPM*) Spectral Estimation:

1. *Section* the data, $\{\mathbf{y}(t)\}$, $t = 1, \ldots, N$ into K sections each of length L, where $K = \frac{N}{L}$, that is,

$$\mathbf{y}_i(t) = \mathbf{y}(t + L(i-1)), \quad i = 1, \ldots, K, \quad t = 0, \ldots, L-1$$

2. *Window* the data to obtain, $\mathbf{y}_i(t) \times \mathcal{W}_i(t)$

3. *Estimate* K periodograms using the DFT as

$$\hat{\mathbf{P}}(\Omega_m, i) = \frac{1}{U}\left|DFT\Big[\mathbf{y}_i(t)\mathcal{W}(t)\Big]\right|^2 \quad i = 1, \ldots, K$$

with $U = \frac{1}{L}\sum_{t=0}^{L-1}\mathcal{W}^2(t)$

4. *Estimate* the average spectrum using

$$\hat{\mathbf{S}}_{yy}(\Omega_m) = \frac{1}{K}\sum_{i=1}^{K}\hat{\mathbf{P}}(\Omega_m, i)$$

with $\text{var}\{\hat{\mathbf{S}}_{yy}(\Omega_m)\} \propto \frac{1}{K}$ and $\text{bias}\{\hat{\mathbf{S}}_{yy}(\Omega_m)\} \propto \frac{K}{N}$ adjusted for particular windows.

3.3 Parametric Multichannel Spectral Estimation: Yule-Walker Method (YWM)

A variety of techniques to estimate discrete multichannel spectral estimators evolved from early seismic work in the 1960's to sophisticated techniques in the 1980's [19]-[22]. These techniques essentially evolved from the lattice methods developed by Robinson and Burg employing the Levinson technique and was extended to the multichannel (output-only) case [19], [20].

The basic spectral relations follow directly from linear systems with random inputs [15]. The measurement of the output spectrum of a process is related to the input spectrum by the factorization relations (in terms of the $\mathcal{Z}$-transform:

$$\mathcal{S}_{yy}(z) = \mathcal{H}(z) \times \mathcal{H}^{\dagger}(z) \times \mathcal{S}_{ee}(z) = |\mathcal{H}(z)|^2 \times \mathcal{S}_{ee}(z) \tag{28}$$

where

$\mathbf{e}$	is the N_y-input process vector (white noise)
$\mathcal{H}$	is the linear system $N_y \times N_y$ transfer function matrix
$\mathbf{y}$	is the N_y-measurement process vector

Since we are taking the output-only viewpoint, then we will assume that *only* the measured data, $\mathbf{y}$, are available and not the excitation, $\mathbf{e}$. In fact, if both e and y are available then the problem is called the system identification problem (see Ljung [23] for details) and the $ARMAX$ model can be used.

In summary, the modern method of *parametric spectral estimation* is given by:

- *Select* the representative model set (AR)
- *Estimate* the model parameters from the data, that is *given* $\{y(t)\}$, *find*

$$\hat{\Theta} = \left\{\hat{\mathcal{A}}(z)\right\} \quad \text{and} \quad \hat{\mathcal{R}}_{ee}$$

- *Estimate* the *PSD* using these parameters, that is,

$$\mathcal{S}_{yy}(z) \approx \hat{\mathcal{S}}_{yy}(z, \hat{\Theta}) = \hat{\mathcal{H}}(z) \times \hat{\mathcal{H}}(z) \times \mathcal{S}_{ee}(z)$$

where $\hat{\mathcal{H}}(z) = \mathcal{A}(z)$ and $\mathcal{S}_{ee}(z) = \hat{\mathcal{R}}_{ee}$

The Yule-Walker method of multichannel spectral estimation is based on solving the following set of linear matrix equations by first redefining the multichannel autoregressive model of Eq. 16 further in terms of the *forward prediction error* as

$$\mathbf{e}_f(t) = \mathbf{a}_{N_a} \times \mathbf{y}(t) \tag{29}$$

where recall

$$\mathbf{a}_{N_a} = \left[\mathbf{I}_{N_a} \;\; \mathbf{A}_{N_a}(1) \cdots \mathbf{A}_{N_a}(N_a)\right]$$

and $\mathbf{y} \in \mathcal{R}^{N_a} \times 1$.

Post-multiplication of this relation and taking the expectation yields [18]

$$E\left\{\mathbf{e}_f(t)\mathbf{y}^\dagger(t)\right\} = E\left\{\mathbf{a}_{N_a} \times \mathbf{y}(t)\mathbf{y}^\dagger(t)\right\} = \mathbf{a}_{N_a} E\left\{\mathbf{y}(t)\mathbf{y}^\dagger(t)\right\} \tag{30}$$

with $\mathbf{R}_{yy}(\ell) \in \mathcal{C}^{N_a N_a}$ a block Toeplitz matrix. Eqn. 30 can be expanded to yield the Yule-Walker equations, that is, expanding we obtain

$$E\left\{\mathbf{e}_f(t)\mathbf{y}^\dagger(t)\right\} = E\left\{\mathbf{e}_f(t) - \sum_{\ell=1}^{N_a} \mathbf{a}_{N_a}(\ell)\mathbf{y}^\dagger(t-\ell)\right\} = [\mathbf{P}_f \;\; \mathbf{0} \;\; \cdots \mathbf{0}] \tag{31}$$

which can be written in vector-matrix form as the multichannel version of the Yule-Walker normal equations:

$$\mathbf{a}_{N_a} \times \mathbf{R}_{yy} = [\mathbf{P}_f \;\; \mathbf{0} \;\; \cdots \mathbf{0}] \tag{32}$$

The *YW* relations enable the extraction of the multichannel (predictor) coefficient matrix and therefore the solution to the multichannel autoregressive power spectrum given by:

$$\mathcal{P}_{AR}(z) = \mathcal{A}^{-1}(z) \times \mathbf{P}_f \times \left(\mathcal{A}^{-1}(z^*)\right)^\dagger \tag{33}$$

The Yule-Walker normal equations can be solved efficiently by the multichannel version of the Levinson recursion (see Refr. [18] for details). Next we consider a suite of lattice-based solutions to the multichannel spectral estimation problem

3.4 Parametric Multichannel Spectral Estimation: Burg Lattice Method (BLM)

The suite of multichannel lattice methods is based on of the *forward* and *backward prediction errors* of the AR-model, defined by

$$\begin{aligned} \mathbf{e}_f(t) &:= \mathbf{y}(t) - \sum_{n=1}^{N} \mathcal{F}(n,N)\mathbf{y}(t-n) \\ \mathbf{e}_b(t) &:= \sum_{n=0}^{N} \mathcal{B}(n,N)\mathbf{y}(t-N+n) \end{aligned} \tag{34}$$

where $\{\mathcal{F}(n,N)\}$ and $\{\mathcal{B}(n,N)\}$ are the respective forward and backward $N \times N$ prediction coefficient matrices.

Minimizing the prediction errors defined by

$$\begin{aligned} \mathbf{P}_f &:= E\Big\{\mathbf{e}_f(t)\mathbf{e}_f^{\dagger}(t)\Big\} = tr\Big[\mathbf{U}_N\Big] \\ \mathbf{P}_b &:= E\Big\{\mathbf{e}_b(t)\mathbf{e}_b^{\dagger}(t)\Big\} = tr\Big[\mathbf{V}_N\Big] \end{aligned} \tag{35}$$

satisfy a set of block-Toeplitz normal equations [18]

$$\begin{bmatrix} \mathbf{I} & \mathcal{F}(1,N) & \cdots & \mathcal{F}(N,N) \\ \\ \mathcal{B}(N,N) & \mathcal{B}(N-1,N) & \cdots & \mathbf{I} \end{bmatrix} \begin{bmatrix} \mathbf{R}(0) & \mathbf{R}^{\dagger}(1) & \cdots & \mathbf{R}^{\dagger}(N) \\ \vdots & \ddots & \vdots & \\ \mathbf{R}(N) & \mathbf{R}(N-1) & \cdots & \mathbf{R}(0) \end{bmatrix} = \begin{bmatrix} \mathbf{U}_N & \mathbf{0} & \cdots & \mathbf{0} \\ \\ \mathbf{0} & \mathbf{0} & \cdots & \mathbf{V}_N \end{bmatrix} \tag{36}$$

The solution to these multichannel equations is given by the Levinson-Wiggins-Robinson (LWR) algorithm recursively relating the set of $(N-1)^{st}$-order coefficients to the $(N)^{th}$-order set, that is, [19], [24]

$$\begin{aligned} \mathcal{K}_N &= \sum_{n=0}^{N-1} \mathcal{F}(N,N-1)\mathbf{R}(N-1) && \text{[Reflection Coeff.]} \\ \mathcal{F}(N,N) &= -\mathcal{K}_N \mathbf{V}_{N-1}^{-1} && \text{[Forward Coeff.]} \\ \mathcal{B}(N,N) &= -\mathcal{K}_N^{\dagger} \mathbf{U}_{N-1}^{-1} && \text{[Backward Coeff.]} \\ \mathbf{U}_N &= \left(\mathbf{I} - \mathcal{F}(N,N)\mathcal{B}(N,N)\right)\mathbf{U}_{N-1} && \text{[Forward Var.]} \end{aligned}$$

$$
\begin{aligned}
\mathbf{V}_N &= (\mathbf{I} - \mathcal{B}(N,N)\mathcal{F}(N,N))\,\mathbf{V}_{N-1} && \text{[Backward Var.]} \\
\mathcal{F}(n,N) &= \mathcal{F}(n,N-1) + \mathcal{F}(N,N)\mathcal{B}(N-n,N) && \text{for} \quad 1 \le n \le N-1 \\
\mathcal{B}(n,N) &= \mathcal{B}(n,N-1) + \mathcal{B}(N,N)\mathcal{F}(N-n,N) && \text{for} \quad 1 \le n \le N-1
\end{aligned}
$$

$$
\text{with} \qquad \mathbf{U}_0 = \mathbf{V}_0 = \mathbf{R}_0; \qquad \mathcal{F}(0,n) = \mathcal{B}(0,n) = \mathbf{I} \qquad \text{for} \qquad 1 \le n \le N-1 \tag{37}
$$

Numerically, the Burg lattice method [20] can have problems because the required covariance matrices may not preserve their positive semi-definite property. Therefore, *Nutall-Strand* (*BLNutS*) approach [22] constrains the calculation to preserve these properties while still employing the *LWR*-algorithm, but altering the computation of the corresponding reflection coefficient $\mathcal{K}$ that is the solution of the *bilinear* equation

$$
\mathbf{V}_{N-1}^{-1} \times \mathbf{P}_b \mathcal{K}_N + \mathcal{K}_N \mathbf{U}_{N-1}^{-1} \mathbf{P}_f = -2\mathbf{R}_{fb}(N) \tag{38}
$$

satisfying a *weighted arithmetic mean* criterion between the forward and backward prediction errors [22].

The *Morf-Viera* (*BLMorfV*) approach (maximum entropy solution) also uses the *LWR*-algorithm, but the reflection coefficient is computed as the *weighted geometric mean* of the forward/backward errors such that [21]

$$
\mathcal{K}_N = \mathbf{U}_{N-1}^{-1/2} \times \mathbf{R}_{fb}(N) \times \mathbf{V}_{N-1}^{-1/2} \tag{39}
$$

where $^{1/2}$ is a matrix square-root (Cholesky decomposition) operation.

The generic multichannel spectrum is given by

$$
\mathcal{P}_{BL}(z) = \mathcal{A}^{-1}(z) \times \mathbf{P}_f \times \left(\mathcal{A}^{-1}(z^*)\right)^\dagger
$$

where $\mathcal{A}^{-1}(z)$ is expressed in terms of either the forward ($\mathcal{F}$) or backward ($\mathcal{B}$) recursions of Eq. 34. This completes the multichannel AR approach providing solutions to the multichannel spectral estimation problem. Next we investigate another alternative technique still based on the underlying multichannel AR-model.

3.5 Multichannel Spectral Estimation: Minimum Variance Method (MVM)

Another approach to multichannel spectral estimation evolves from the array signal processing literature [13] where the multichannel "spatial" power spectrum is estimated. Here the minimum variance or to be more precise *minimum variance distortionless response* technique (see [18] for details) has evolved. It is based on the idea constraining the processor to pass a narrowband frequency (distortionless response) while minimizing the power (minimum variance) of those frequencies outside of the narrow band. It can be calculated directly from the inverse covariance matrix as

$$\mathbf{S}_{MV}(\Omega) := \triangle t \left[\mathbf{e}(\Omega)\mathcal{R}^{-1}\mathbf{e}^{\dagger}(\Omega)\right]^{-1}$$

where $\mathcal{R}$ is the block Toeplitz matrix (as before) and $\mathbf{e}$ is a block complex sinusoidal vector defined by []

$$\mathbf{e}(z) := \left[I_m \;\; e^{j\Omega_m \triangle t} I_m \cdots \;\; e^{j\Omega_m N_a \triangle t} I_m\right]$$

An alternative approach is based on using the multichannel AR-model such that [18]

$$\hat{\mathbf{S}}_{MV}(\Omega) = \triangle t \Big[\sum_{\ell=-N_a}^{N_a} \Theta(\ell) e^{j\Omega_\ell \triangle t}\Big]^{-1}$$

where

$$\Theta(\ell) = \begin{cases} \triangle t \sum_{i=0}^{N_a-\ell} \left\{(N_a+1-\ell-i)\mathcal{A}^{\dagger}(\ell+i)\mathbf{P}_f^{-1}\mathcal{A}(i) - i\mathcal{B}^{\dagger}(\ell+i)\mathbf{P}_b^{-1}\mathcal{B}(i)\right\} & \text{for } 0 \le \ell \le N_a \\ \Theta^{\dagger}(-\ell) & \text{for } -1 \le \ell \le -N_a \end{cases}$$

Next we consider a different approach to solving this problem using the multichannel state-space representation leading to a "model-based" solution.

3.6 Multichannel Spectral Estimation: State-Space Approach

We start with the innovations (INV) state-space model and investigate its properties leading to the multichannel spectral representation. Note that it is equivalent to the steady-state Kalman filter for stationary processes, that is, the innovations representation of the Kalman filter in "prediction form" is given by (see [24] for details)

$$\begin{array}{rcll} \hat{x}(t+1) & = & A\hat{x}(t) + K_p(t)e(t) & \text{[State Estimate]} \\ y(t) & = & C\hat{x}(t) + e(t) & \text{[Measurement]} \\ \hat{y}(t) & = & C\hat{x}(t) & \text{[Measurement Estimate]} \\ e(t) & = & y(t) - \hat{y}(t) & \text{[Innovation]} \end{array} \tag{40}$$

where $e(t)$ is the innovation sequence and $K_p(t)$ is the *predicted Kalman gain* for correlated noise sources $\text{cov}(w, v)$ with state error covariance $\tilde{P}(t)$ given by

$$\begin{array}{rcll} R_{ee}(t) & = & C\tilde{P}(t)C' + R_{vv}(t) & \text{[Innovations Covariance]} \\ K_p(t) & = & (A\tilde{P}(t)C' + R_{wv}(t))R_{ee}^{-1}(t) & \text{[Kalman Gain]} \\ \tilde{P}(t+1) & = & A\tilde{P}(t)A' - K_p(t)R_{ee}(t)K_p'(t) + R_{ww}(t) & \text{[Error Covariance]} \end{array} \tag{41}$$

and we have used the simplified notation: $\hat{x}(t+1|t) \rightarrow \hat{x}(t+1)$ and $\tilde{P}(t+1|t) \rightarrow \tilde{P}(t+1)$.

In terms of this model, the "transfer function" of the *INV*-model is defined by

$$T(z) := \frac{Y(z)}{E(Z)} = C(zI - A)^{-1}K_p \tag{42}$$

Calculating the measurement covariance corresponding to Σ_{INV}, when svd

$$y(t) = e(t) + \hat{y}(t)$$

gives

$$R_{yy}(\ell) = \text{cov}[y(t+\ell)y(t)] = R_{\hat{y}\hat{y}}(\ell) + R_{\hat{y}e}(\ell) + R_{e\hat{y}}(\ell) + R_{ee}(\ell) \tag{43}$$

Taking the $\mathcal{Z}$-transform of this relation, we obtain the multichannel (measurement) *PSD* in terms of the innovations model as

$$S_{yy}(z) = S_{\hat{y}\hat{y}}(z) + S_{\hat{y}e}(z) + S_{e\hat{y}}(z) + S_{ee}(z) \tag{44}$$

where

$$\begin{array}{rcl} S_{\hat{y}\hat{y}}(z) & = & CS_{\hat{x}\hat{x}}(z)C' = T(z)S_{ee}(z)T'(z^{-1}); \quad S_{ee}(z) = R_{ee} \\ S_{\hat{y}e}(z) & = & CS_{\hat{x}e}(z) = T(z)S_{ee}(z); \quad \text{and} \quad S_{e\hat{y}}(z) = S_{ee}(z)T'(z^{-1}) \end{array} \tag{45}$$

Thus, the multichannel *PSD* of the state-space (innovations) model is given by

$$S_{yy}(z) = T(z)S_{ee}(z)T'(z^{-1}) + T(z)S_{ee}(z) + S_{ee}(z)T'(z^{-1}) + S_{ee}(z) \tag{46}$$

Substituting for $T(z)$ and replacing $S_{ee}(z) = R_{ee}$, the measurement power spectrum can be expressed as

$$S_{yy}(z) := \mathcal{H}_e(z) \times \mathcal{H}'_e(z^{-1}) = [T(z)R_{ee}^{1/2} \mid R_{ee}^{1/2}] \times \begin{bmatrix} (R_{ee}^{1/2})'T'(z^{-1}) \\ - - - \\ (R_{ee}^{1/2})' \end{bmatrix} \text{ [Spectral Factors]} \tag{47}$$

Next, we must show how the *INV*-model (Kalman filter) relates to the Kalman filter parameters in order to specify a stochastic realization. Therefore, the model set for the innovations model is defined as

$$\Sigma_{INV} := \{A, B, C, D, K_p, R_{ee}\}$$

The *stationary measurement covariance* at lag ℓ is given by

$$\Lambda_\ell = \begin{cases} \underbrace{C}_{\tilde{C}} \underbrace{A^{\ell-1}}_{\tilde{A}} \underbrace{\left(A\tilde{\Pi}C' + K_p R_{ee}\right)}_{\tilde{B}} & \text{for} \quad \ell > 0 \\ C\underbrace{\tilde{\Pi}C' + R_{ee}}_{\tilde{D}+\tilde{D}'} & \text{for} \quad \ell = 0 \\ \Lambda_{yy}(-\ell) & \text{for} \quad \ell < 0 \end{cases} \tag{48}$$

where $\tilde{\Sigma}_{KSP} = \{\tilde{A}, \tilde{B}, \tilde{C}, \tilde{D}\}$ is the underlying Kalman-Szego-Popov (*KSP*) model [26].

The solution can be stated formally as:

GIVEN a minimal realization $\tilde{\Sigma}_{KSP}$ of $\{\Lambda_\ell\}$, THEN the model set $\{\tilde{A}, \tilde{B}, \tilde{C}, \tilde{D}, \tilde{\Pi}\}$ is a *stochastic realization* of the measurement sequence, if there exists a $\tilde{\Pi} \geq 0$ such that the following *KSP equations* are satisfied:

$$\begin{aligned} \tilde{\Pi} - \tilde{A}\ \tilde{\Pi}\ \tilde{A}' &= K_p\ R_{ee}\ K_p' \\ \tilde{B} - \tilde{A}\ \tilde{\Pi}\tilde{C}' &= K_p\ R_{ee} \\ \tilde{D} + \tilde{D}' - \tilde{C}\ \tilde{\Pi}\ \tilde{C}' &= R_{ee} \end{aligned} \tag{49}$$

Solving for K_p in the second *KSP*-equation of Eq. 49 and substituting the last equation for the innovations covariance R_{ee} yields

$$K_p = (\tilde{B} - \tilde{A}\ \tilde{\Pi}\ \tilde{C}') \times (\tilde{D} + \tilde{D}' - \tilde{C}\ \tilde{\Pi}\ \tilde{C}')^{-1} \tag{50}$$

Substituting these expressions into the first equation of Eq. 49 above shows that the state error covariance $\tilde{\Pi}$ satisfies a discrete *Riccati equation*, that is,

$$\tilde{\Pi} = \tilde{A}\tilde{\Pi}\tilde{A}' + (\tilde{B}\tilde{A}\tilde{\Pi}\tilde{C}')(\tilde{D} + \tilde{D}' - \tilde{C}\tilde{\Pi}\tilde{C}')^{-1}(\tilde{B} - \tilde{A}\tilde{\Pi}\tilde{C}')' \quad \text{[Riccati Equation]} \tag{51}$$

guaranteeing a proper stochastic realization($\tilde{\pi} > 0$).

Any deterministic realization algorithm applied to $\{\Lambda_\ell\}$ such that the following Hankel factorization yields a reasonable approach to extract the *KSP* relations evolving from the innovations model. For instance, the well-known, classical Ho-Kalman *SVD*-approach [25] can be applied to give

$$\begin{aligned} \Lambda_{K,K} &= \mathcal{O}_K \times \overline{\mathcal{C}}_k \\ &= \underbrace{\begin{bmatrix} C \\ CA \\ \vdots \\ CA^{K-2} \end{bmatrix}}_{\mathcal{O}_K} \underbrace{\begin{bmatrix} A\Pi C' \mid A^2\Pi C' \mid \cdots \mid A^{K-1}\Pi C' \end{bmatrix}}_{\overline{\mathcal{C}}_K} \end{aligned} \tag{52}$$

Once the $\tilde{\Sigma}_{KSP}$ model is estimated from the covariance sequence, then the *KSP*-equations can be solved to complete the stochastic realization, that is,

$$\begin{aligned} R_{ee} &= \tilde{D} + \tilde{D}' - \tilde{C}\ \tilde{\Pi}\ \tilde{C}' \\ K_p &= (\tilde{B} - \tilde{A}\ \tilde{\Pi}\ \tilde{C}') \times R_{ee}^{-1} \end{aligned} \tag{53}$$

We summarize this approach as:

- *Perform* a realization (deterministic) to obtain $\tilde{\Sigma}_{KSP}$
- *Solve* the Riccati equation of Eq. 51 to obtain $\tilde{\Pi}$
- *Calculate* R_{ee} and K from the *KSP*-equations of Eq. 53

Thus, we see that performing a deterministic realization from a Hankel matrix populated by the covariance sequence $\{\Lambda_\ell\}$ yields the model $\tilde{\Sigma}_{KSP}$ that is used to estimate $\tilde{\Pi}$ from the corresponding Riccati equation giving the corresponding Kalman gain and innovations covariance [26].

A numerically efficient approach to solving this "output-only", multichannel spectral estimation problem is to apply *subspace* methods directly to the data. Subspace methods applied to the output-only problem, perform an orthogonal projection in a Hilbert space occupied by random vectors [26]. That is, if $\mathbf{y}_f(t)$ is a finite random vector of *future* outputs and $\mathbf{y}_p(t)$ a random vector of *past* outputs, then the *orthogonal projection* of the "future output data onto the past output data" is defined by $\mathcal{P}_{y_f|y_p}$. We define the following block Hankel matrices for future and past data as:

$$\mathcal{Y}_f = \begin{bmatrix} \mathbf{y}(k) & \cdots & \mathbf{y}(K+k-1) \\ \vdots & \vdots & \vdots \\ \mathbf{y}(2k-1) & \cdots & \mathbf{y}(K+2k-2) \end{bmatrix} \qquad \text{[FutureData]}$$

$$\mathcal{Y}_p = \begin{bmatrix} \mathbf{y}(0) & \cdots & \mathbf{y}(K-1) \\ \vdots & \vdots & \vdots \\ \mathbf{y}(k-1) & \cdots & \mathbf{y}(K+k-2) \end{bmatrix} \qquad \text{[PastData]}$$

An orthogonal projection of the row space of future data $\mathcal{Y}_f$ onto the row space of past data $\mathcal{Y}_p$ is given by [27], [28]

$$\mathcal{P}_{\mathcal{Y}_f|\mathcal{Y}_p} = \mathcal{Y}_f \times \mathcal{P}_{\bullet|\mathcal{Y}_p} = \underbrace{E\{\mathcal{Y}_f\mathcal{Y}_p'\}}_{\mathbf{T}_k} \times \underbrace{E\{\mathcal{Y}_p\mathcal{Y}_p'\}}_{\mathcal{T}_k}^{-1} \times \mathcal{Y}_p = \mathbf{T}_k \times \mathcal{T}_k^{-1} \times \mathcal{Y}_p \tag{54}$$

where the underlying matrices are defined in terms of block Toeplitz covariance matrices, that is,

$$\mathbf{T}_k := E\{\mathcal{Y}_f \mathcal{Y}_p'\} = \begin{bmatrix} \Lambda_k & \cdots & \Lambda_1 \\ \vdots & \ddots & \vdots \\ \Lambda_{2k-1} & \cdots & \Lambda_k \end{bmatrix} \in \mathcal{R}^{kN_y \times kN_y} \tag{55}$$

with the data assumed to be generated by the *innovations model* and measurement output covariance given by

$$\Lambda_\ell = CA^{\ell-1} \underbrace{(A\hat{\Pi}C' + K_p R_{ee})}_{\overline{B}_e}$$

Therefore, we obtain a factorization similar to that of deterministic realization theory [25]

$$\begin{aligned} \mathbf{T}_k &= \begin{bmatrix} CA^{k-1}\overline{B}_e & \cdots & C\overline{B}_e \\ \vdots & \ddots & \vdots \\ CA^{2k-2}\overline{B}_e & \cdots & CA^{k-1}\overline{B}_e \end{bmatrix} \in \mathcal{R}^{kN_y \times kN_y} \\ &= \underbrace{\begin{bmatrix} C \\ \vdots \\ CA^{k-1} \end{bmatrix}}_{\mathcal{O}_k} \underbrace{\begin{bmatrix} A^{k-1}\overline{B}_e \mid \cdots \mid \overline{B}_e \end{bmatrix}}_{\overline{\mathcal{C}}^{\leftarrow}_{AB}(k)} \end{aligned} \tag{56}$$

given by the product of the *observability* matrix and the *reversed controllability* matrix

$$\mathbf{T}_k = \mathcal{O}_k \times \overline{\mathcal{C}}^{\leftarrow}_{AB}(k) \tag{57}$$

The block Toeplitz matrix of the projection $\mathcal{T}_k$ is

$$\mathcal{T}_k = E\{\mathcal{Y}_p \mathcal{Y}_p'\} = \begin{bmatrix} \Lambda_0 & \cdots & \Lambda_{1-k} \\ \vdots & \ddots & \vdots \\ \Lambda_{k-1} & \cdots & \Lambda_0 \end{bmatrix} \in \mathcal{R}^{kN_y \times kN_y} \tag{58}$$

Using the innovations model, it has been shown that the augmented state vector

$$\hat{\mathcal{X}}_k := [\hat{\mathbf{x}}_k \;\; \hat{\mathbf{x}}_{k+1} \;\; \cdots \;\; \hat{\mathbf{x}}_{K+k-1}] \in \mathcal{R}^{N_x \times KN_x}$$

satisfies the following relation [29], [30]

$$\hat{\mathcal{X}}_k \;\; = \;\; \overline{\mathcal{C}}^{\leftarrow}_{AB}(k) \times \mathcal{T}_k^{-1} \times \mathcal{Y}_p \tag{59}$$

and therefore, incorporating this expression into the orthogonal projection, we obtain

$$\mathcal{P}_{\mathcal{Y}_f|\mathcal{Y}_p} = \mathbf{T}_k \times \mathcal{T}_k^{-1} \times \mathcal{Y}_p = \mathcal{O}_k \; \underbrace{\overline{\mathcal{C}}^{\leftarrow}_{AB}(k) \times \mathcal{T}_k^{-1} \times \mathcal{Y}_p}_{\hat{\mathcal{X}}_k} = \mathcal{O}_k \times \hat{\mathcal{X}}_k \tag{60}$$

Thus, both the extended observability matrix as well as the estimated state vectors can be extracted by performing the singular value decomposition of the orthogonal projection matrix, that is,

$$\mathcal{P}_{\mathcal{Y}_f|\mathcal{Y}_p} = \begin{bmatrix} U_{N_x} \mid U_{\mathcal{N}} \end{bmatrix} \begin{bmatrix} \Sigma_{N_x} & | & 0 \\ - & - & - \\ 0 & | & \Sigma_{\mathcal{N}} \end{bmatrix} \begin{bmatrix} V'_{N_x} \\ -- \\ V'_{\mathcal{N}} \end{bmatrix} = U_{N_x} \Sigma_{N_x} V'_{N_x}$$

where $\Sigma_{N_x} >> \Sigma_{\mathcal{N}}$ and

$$\mathcal{P}_{\mathcal{Y}_f|\mathcal{Y}_p} = \mathcal{O}_k \hat{\mathcal{X}}_k = \underbrace{\left(U_{N_x} \Sigma_{N_x}^{1/2}\right)}_{\mathcal{O}_{N_x}} \underbrace{\left((\Sigma'_{N_x})^{1/2} V'_{N_x}\right)}_{\hat{\mathcal{X}}_k} \tag{61}$$

With the singular value decomposition available, we exploit the projection to extract the system and output measurement matrices [26], [33]

$$\hat{A} = \mathcal{O}_{N_x}^{\#} \mathcal{O}_{N_x}^{\uparrow} = (\Sigma_{N_x}^{-1/2} U'_{N_x}) \times \mathcal{O}_{N_x}^{\uparrow}; \qquad \hat{C} = \mathcal{O}(1 : N_y, 1 : N_x) \tag{62}$$

where $\mathcal{O}_{N_x}^{\uparrow}$ is the observability matrix "shifted-up" one row and $^{\#}$ is the pseudo-inverse.

The input transmission matrix ($\overline{B}_e$) can be extracted by first estimating the reversed controllability matrix from Eq. 57

$$\overline{\mathcal{C}}_{AB}^{\leftarrow}(k) = \mathcal{O}_{N_x}^{\#} \times \mathbf{T}_{k,k} = (\Sigma_{N_x}^{-1/2} U'_{N_x}) \times \mathbf{T}_{k,k} \tag{63}$$

and extracting the last k-columns to obtain

$$\hat{B} = \overline{B}_e = \overline{\mathcal{C}}_{AB}^{\leftarrow}(1 : N_x, (k-1)N_y : kN_y) \tag{64}$$

The input-output transmission matrix is obtained from the sample covariance estimate of $\hat{\Lambda}_0$

$$\hat{D} = \hat{\Lambda}_0 \tag{65}$$

With the $\hat{\Sigma}_{KSP} = \{\hat{A}, \hat{B}, \hat{C}, \hat{D}\}$ model now available, we can solve the Riccati equation to obtain $\hat{\Pi} > 0$ and extract the remaining matrices to provide a solution to the "output-only" stochastic realization problem.

Thus,, the *"output-only" subspace stochastic realization* (*OO-SID*)[5] algorithm is accomplished using the following steps:

- *Create* the block Hankel matrix from the measured output sequence, $\{\mathbf{y}(t)\}$;
- *Calculate* the orthogonal projection matrix $\mathcal{P}_{\mathcal{Y}_f|\mathcal{Y}_p}$ as in Eq. 54 ;

[5]For structural dynamic systems only the system (A) and measurement (C) matrices are required to extract the modal frequencies and shapes [31], [32].

- *Perform* the *SVD* of the projection matrix to obtain the extended observability and estimated state vectors in Eq. 61;
- *Extract* the system matrix $\hat{A}$ and output $\hat{C}$ matrices as in Eq. 62;
- *Calculate* the reversed controllability matrix $\overline{\mathcal{C}}_{AB}^{\leftarrow}$ as in Eq. 63;
- *Extract* the input transmission matrix $\hat{B}$ as in Eq. 64;
- *Extract* the input/output matrix $\hat{D}$ from estimated output covariance $\hat{\Lambda}_0$;
- *Solve* the corresponding Riccati equation of Eq. 51 using $\Sigma_{KSP} = \{\hat{A}, \hat{B}, \hat{C}, \hat{D}\}$ to obtain $\hat{\Pi}$; and
- *Calculate* R_{ee} and K_p from the *KSP*-equations of Eq. 49.

This completes the development of the output-only subspace identification algorithm, next we consider the structural dynamics problem of interest for multichannel spectral estimators.

4 Vibrational Systems

Vibrational systems operating over long periods of time can be subjected to anomalies due to fatigue caused various external forces. Standard approaches to detect anomalous mechanisms at the onset range from a simple accelerometer strategically placed to observe the Fourier spectrum of known response to using cepstral analysis to identify periodic responses. Measures of anomalies can deteriorate significantly if noise is present - a common situation in an operational environment. Most of the current monitoring approaches for anomaly detection and isolation lead to single-channel processing of measured sensor data. Multiple sensors (such as accelerometers for vibrations, microphones for acoustics, strain gauges for stress and thermocouples for temperature) in a structure provide enhanced information about the system for condition and performance. This implies that the application of a multichannel (multi-input, multi-output) system representation is required. This section is based on developing a model-based signal processing approach to solve the vibrational system multichannel power spectral estimation problem.

Model-based signal processing for structures involves incorporation of the process model (large-scale structure), measurement model (wireless sensor network), and noise models (instrumentation, environmental, parameter uncertainty, etc.) along with measured data into a sophisticated processing algorithm capable of detecting, filtering (estimating), and isolating a mechanical fault in a hostile operational environment. The model-based processor (*MBP*) provides estimates of various quantities of high interest (modes, vibrational response, resonances, etc.), as well as on-line statistical performance measures.

4.1 Single Input/Single Output (*SISO*) Mechanical Systems

Suppose we have a simple mass (m), damping (c), spring (k), mechanical system (MCK) driven by an external forcing function. The dynamics of this system can be expressed in terms of a second-order *differential equation* in continuous-time τ as

$$m\ddot{d}(\tau) + c\dot{d}(\tau) + kd(\tau) = p(\tau) \tag{66}$$

This system can also be expressed as a *transfer function* by applying Laplace transforms $\mathcal{L}[d(\tau)] := D(s)$ to give

$$ms^2D(s) + csD(s) + kD(s) = P(s) \tag{67}$$

Factoring out $D(s)$, dividing through by m and solving, leads to the continuous-time *transfer function* representation

$$\mathcal{H}(s) := \frac{D(s)}{P(s)} = \frac{1/m}{s^2 + c/ms + k/m} \tag{68}$$

This simple system can be placed in *state-space* form by defining the state vector $\mathbf{x}(\tau) := [d(\tau) \mid \dot{d}(\tau)]'$ and rewriting the second-order differential equation of Eq. 66 in terms of two first-order differential equations as

$$\begin{aligned} \dot{x}_1(\tau) &= x_2(\tau) \\ \dot{x}_2(\tau) &= -\frac{k}{m}x_1(\tau) - \frac{c}{m}x_2(\tau) \\ \text{with output} & \\ y(\tau) &= x_1(\tau) \end{aligned} \tag{69}$$

or equivalently in matrix-vector format, we obtain

$$\begin{aligned} \dot{\mathbf{x}}(\tau) &= \begin{bmatrix} 0 & -1 \\ -\frac{k}{m} & -\frac{c}{m} \end{bmatrix} \mathbf{x}(\tau) + \mathbf{p}(\tau) \\ y(\tau) &= \begin{bmatrix} 1 & 0 \end{bmatrix} \mathbf{x}(\tau) \end{aligned} \tag{70}$$

More generally we can express the multiple input/multiple output (MIMO) *state-space system* by the quadruple $\Sigma := (A, B, C, D)$ given by

$$\begin{aligned} \dot{\mathbf{x}}(\tau) &= A\mathbf{x}(\tau) + B\mathbf{u}(\tau) \\ \mathbf{y}(\tau) &= C\mathbf{x}(\tau) + D\mathbf{u}(\tau) \end{aligned} \tag{71}$$

where the state-vector is $\mathbf{x} \in \mathcal{R}^{N_x \times 1}$, the known input excitation is $\mathbf{u} \in \mathcal{R}^{N_u \times 1}$ and the output is $\mathbf{y} \in \mathcal{R}^{N_y \times 1}$ with corresponding system matrices given by the state transition matrix, $A \in \mathcal{R}^{N_x \times N_x}$, the input transmission matrix, $B \in \mathcal{R}^{N_x \times N_u}$, output matrix $C \in \mathcal{R}^{N_y \times N_x}$ and the input-output transmission matrix $D \in \mathcal{R}^{N_y \times N_u}$.

From the mechanical system perspective we can also factor the denominator of transfer function of Eq. 68 and we see that it can be represented equivalently in the generic modal form and its corresponding partial fraction form as

$$\mathcal{H}(s) = \frac{2\Re[R]s + 2\Re[R]\sigma - 2\omega\Im[R]}{s^2 + 2\sigma s + (\sigma^2 + \omega^2)} = \frac{R}{s + \sigma - j\omega} + \frac{R^*}{s + \sigma + j\omega} \tag{72}$$

where $\Re[\cdot]$ is the real part of $[\cdot]$, $\Im[\cdot]$ is its imaginary part and R its residue.

Performing the inverse Laplace transform of this relation, we obtain the corresponding modal representation

$$\mathcal{H}(\tau) = Re^{-(\sigma + j\omega)} + R^* e^{-(\sigma - j\omega)} \tag{73}$$

with modes or poles given by $-\sigma \pm j\omega$ and residues or mode shapes by R.

Relating back to a physical system, the generic second-order system (control theory) has a transfer function of the form

$$\mathcal{H}(s) = \frac{\omega_n^2}{s^2 + 2\zeta\omega_n s + \omega_n^2} = \frac{\omega_n^2}{(s + \zeta\omega_n - j\omega_n\sqrt{1-\zeta^2})(s + \zeta\omega_n + j\omega_n\sqrt{1-\zeta^2})} \tag{74}$$

where ω_n is the *undamped natural frequency* and ζ is the *damping ratio* of the system. In terms of our modal interpretation of Eq. 72, we have that

$$\begin{aligned} \sigma &= \zeta\omega_n \\ \omega &= \omega_n\sqrt{1-\zeta^2} \end{aligned} \tag{75}$$

and σ is called the *damping coefficient* with ω termed the *damped natural frequency*. The system *time constant* is also defined as

$$\tau_c = \frac{1}{\sigma} = \frac{1}{\zeta\omega_n}$$

completing the analogy. Solving the second-order equation using the inverse Laplace transform leads to the real impulse response of a damped sinusoid

$$\mathcal{H}(\tau) = K_\tau e^{-\sigma\tau}\sin(\omega\tau + \phi) = K_\tau e^{-\zeta\omega_n\tau}\sin(\omega_n\sqrt{1-\zeta^2}\tau + \phi) \tag{76}$$

Now placing the modal model into single-input/single output (*SISO*) state-space form, we have

$$\begin{aligned}\dot{\mathbf{x}}(\tau) &= A_M\mathbf{x}(\tau) + \mathbf{b}_M\mathbf{u}(\tau)\\ \mathbf{y}(\tau) &= \mathbf{c}_M\mathbf{x}(\tau) + \mathbf{d}_M\mathbf{u}(\tau)\end{aligned} \tag{77}$$

where the system matrices become [15]

$$A_M = \begin{bmatrix} \sigma_i & \omega_i \\ -\omega_i & \sigma_i \end{bmatrix}; \mathbf{b}_M = \begin{bmatrix} 2\Im[R_i] \\ 2\Re[R_i] \end{bmatrix};\ \mathbf{c}_M = \begin{bmatrix} 0 & 1 \end{bmatrix} \text{ and } \mathbf{d}_M = \mathbf{d}$$

which is a special case of the general state-space model that can be extended to multiple input/multiple output vibrational systems to follow next.

4.2 Multiple Input/Multiple Output (*MIMO*) Mechanical Systems

Multichannel spectral estimation is based on an "output-only" concept especially in vibration testing where the input excitation is assumed to be random and uncorrelated (white). Here we investigate the *MIMO* formulation of the system and show its direct relationship to the state-space representation as well as convenient coordinates for analysis.

A linear, time-invariant mechanical system can be characterized by

$$M\ddot{\mathbf{d}}(\tau) + C_d\dot{\mathbf{d}}(\tau) + K\mathbf{d}(\tau) = B_p\mathbf{p}(\tau) \tag{78}$$

where $\mathbf{d}$ is the $N_d \times 1$ displacement vector, $\mathbf{p}$ is the $N_p \times 1$ excitation force, and M, C_d, K, are the $N_d \times N_d$ lumped mass, damping, and spring constant matrices characterizing the vibrational process model, respectively. The structure of these matrices, typically, take the form as

$$M = \begin{bmatrix} M_1 & 0 & 0 & 0 & 0 \\ 0 & M_2 & 0 & 0 & 0 \\ \vdots & \vdots & \ddots & \vdots & \vdots \\ 0 & 0 & 0 & M_{N_d-1} & 0 \\ 0 & 0 & 0 & 0 & M_{N_d} \end{bmatrix}, \qquad C_d = \begin{bmatrix} C_{d_{ij}} \end{bmatrix}, \quad \text{and}$$

$$K = \begin{bmatrix} (K_1+K_2) & -K_2 & 0 & 0 & 0 \\ -K_2 & (K_2+K_3) & \ddots & 0 & 0 \\ 0 & \ddots & \ddots & -K_{N_d-1} & 0 \\ 0 & 0 & -K_{N_d-1} & (K_{N_d-1}+K_{N_d}) & -K_{N_d} \\ 0 & 0 & 0 & -K_{N_d} & K_{N_d} \end{bmatrix}$$

If we define the $2N_d$-state vector as $\mathbf{x}(\tau) := \begin{bmatrix} \mathbf{d}(\tau) & | & \dot{\mathbf{d}}(\tau) \end{bmatrix}$, then the continuous-time state-space representation of this process can be expressed as

$$\dot{\mathbf{x}}(\tau) \;=\; \underbrace{\left[\begin{array}{c|c} 0 & I \\ \hline -M^{-1}K & -M^{-1}C_d \end{array}\right]}_{A}\mathbf{x}(\tau) + \underbrace{\left[\begin{array}{c} 0 \\ \hline M^{-1}B_p \end{array}\right]}_{B}\mathbf{p}(t) \tag{79}$$

The corresponding measurement or output vector relation can be characterized by

$$\mathbf{y}(\tau) = \mathbf{C_a}\ddot{\mathbf{d}}(\tau) + \mathbf{C_v}\dot{\mathbf{d}}(\tau) + \mathbf{C_d}\mathbf{d}(\tau) \tag{80}$$

where the constant matrices: $\mathbf{C_a}, \mathbf{C_v}, \mathbf{C_d}$ are the respective acceleration, velocity and displacement weighting matrices of appropriate dimension.

In terms of the state vector relations of Eq. 79, we can express the acceleration vector as:

$$\ddot{\mathbf{d}}(\tau) = -M^{-1}K\mathbf{d}(\tau) - M^{-1}C_d\dot{\mathbf{d}}(\tau) + M^{-1}B_p\mathbf{p}(\tau) \tag{81}$$

Substituting for the acceleration term in Eq. 80, we have that

$$\mathbf{y}(\tau) = -\mathbf{C_a}M^{-1}\Big[B_p\mathbf{p}(\tau) - C_d\dot{\mathbf{d}}(\tau) - K\mathbf{d}(\tau)\Big] + \mathbf{C_v}\dot{\mathbf{d}}(\tau) + \mathbf{C_d}\mathbf{d}(\tau)$$

or

$$\mathbf{y}(\tau) = \underbrace{\Big[C_d - \mathbf{C_a}M^{-1}K \;\Big|\; \mathbf{C_v} - \mathbf{C_a}M^{-1}\mathbf{C_d}\Big]}_{C}\left[\begin{array}{c} \mathbf{d}(\tau) \\ \hline \dot{\mathbf{d}}(\tau \end{array}\right] + \underbrace{\mathbf{C_a}M^{-1}B_p}_{D}\,\mathbf{p}(\tau) \tag{82}$$

to yield the vibrational measurement as:

$$\mathbf{y}(\tau) = C\mathbf{x}(\tau) + D\mathbf{u}(\tau) \tag{83}$$

where the output or measurement vector is $\mathbf{y} \in \mathcal{R}^{N_y \times 1}$ completing the multiple input/multiple output (*MIMO*) vibrational model.

Note that sensor models can capture the dynamics of the sensors, as they interact with the dynamics of the states. For example, in a typical vibrational system, this equation represents the outputs of a set of accelerometers which are wideband relative to the process and therefore, simply fixed gains.

4.3 Modal State-Space Model

Perhaps one of the most expository representations of a mechanical system is its modal representation [4], [5], where the modes and mode shape expose the internal structure and its response to various excitations. The modal representation of a system can easily be

found from state-space systems by transforming the coordinates of the representation to modal space which is accomplished through an eigen-decomposition in the form of a so-called *similarity transformation* such that the system matrices $\Sigma := \{A, B, C\}$ are transformed to modal coordinates by the transformation matrix T_M constructed of the eigenvectors of the underlying system [10],[11], that is,

$$\Sigma \quad \overset{T_M}{\longrightarrow} \quad \Sigma_M$$

where we have

$$\Big\{A, B, C, D\Big\} \longrightarrow \Big\{A_M, B_M, C_M, D_M\Big\} := \Big\{T_M A T_M^{-1}\ , T_M B,\ CT_M^{-1}, D\Big\}$$

that yields an "equivalent" system from an input/output perspective, that is, the transfer functions are identical

$$H(s) = C_M(sI - A_M)^{-1}B_M + D_M = CT_M^{-1} \times (sI - T_M A T_M^{-1})^{-1} \times T_M B = C(sI - A)^{-1}B + D$$

as well as the corresponding impulse response matrices

$$H(\tau) = C_M e^{A_M(\tau)} B_M = CT_M^{-1} \times T_M e^{A(\tau)} T_M^{-1} \times T_M B = Ce^{A(\tau)}B$$

It is well-known from systems theory [10], [11] that the solution to the continuous-time, state-space system of Eq. 71 is given by

$$\mathbf{x}(\tau) = \underbrace{e^{A(\tau-\tau_0)}\mathbf{x}(\tau_0)}_{\text{homogeneous}} + \underbrace{\int_{\tau_0}^{\tau} e^{A(\tau-\alpha)} B\mathbf{u}(\alpha)d\alpha}_{\text{forced}} \tag{84}$$

consisting of the homogeneous and forced solutions from which can define the *state transition matrix* for the linear time invariant (LTI) system as

$$\mathbf{\Phi}(\tau, \tau_0) = e^{A(\tau-\tau_0)} \qquad \text{[State Transition Matrix]} \tag{85}$$

Transforming this solution by performing an eigen-decomposition for distinct (independent) eigenvalues leads to a diagonal transition matrix, that is, selecting the modal similarity transformation T_M for

$$x(\tau) = T_M \times x_M(\tau)$$

satisfying the eigen-equations

$$A\varepsilon_i = \lambda_i \varepsilon_i \qquad \text{for} \qquad i = 1, 2, \cdots, N_x$$

where $\{\lambda_i\}$ are the distinct eigenvalues (real and/or complex) of A or equivalently the roots (modes) of the determinant $|\lambda I - A|$ (characteristic equation) [10] and $\{\varepsilon_i\}$ are the corresponding eigenvectors (mode shapes) that lead to

$$T_M = [\varepsilon_1 \mid \varepsilon_2 \mid \cdots \mid \varepsilon_{N_x}]$$

the *modal matrix* consisting of independent columns such that

$$AT_M = T_M\Lambda$$

for $\Lambda = \text{diag}[\lambda_1, \lambda_2, \cdots, \lambda_{N_x}]$.

For this modal system, we have that the *modal* state transition matrix $\mathbf{\Phi}_M$ follows from the eigen-decomposition as

$$\mathbf{\Phi}_M(\tau, \tau_0) = T_M e^{A(\tau-\tau_0)} T_M^{-1} = e^{T_M A(\tau-\tau_0)T_M^{-1}} = e^{\Lambda(\tau-\tau_0)} = \sum_{i=1}^{N_x} \varepsilon_i e^{\lambda_i(\tau-\tau_0)} \eta_i^T \tag{86}$$

where we have incorporated the *reciprocal eigenvectorss* $\{\eta_i^T\};\ i = 1, \cdots, N_x$ (rows of T_M^{-1}) to obtain

$$\mathbf{\Phi}_M(\tau, \tau_0) = e^{\Lambda(\tau-\tau_0)} = \begin{bmatrix} e^{\lambda_1(\tau-\tau_0)} & & 0 \\ & \ddots & \\ 0 & & e^{\lambda_{N_x}(\tau-\tau_0)} \end{bmatrix} \quad \text{[MODAL State Transition Matrix]} \tag{87}$$

In this coordinate system, the *modal* state solution is:

$$\mathbf{x}_M(\tau) = e^{\Lambda(\tau-\tau_0)}\mathbf{x}_M(\tau_0) + \int_{\tau_0}^{\tau} e^{\Lambda(\tau-\alpha)} B\mathbf{u}(\alpha)d\alpha \tag{88}$$

which can be written explicitly for the i^{th}-mode x_i as

$$x_i(\tau) = e^{\lambda_i(\tau-\tau_0)}x_i(\tau_0) + \int_{\tau_0}^{\tau} e^{\lambda_i(\tau-\alpha)} b_{im}u_m(\alpha)d\alpha \text{ for } i = 1, 2, \cdots, N_x; m = 1, \cdots, N_u \tag{89}$$

with b_{im} the $(i, m)^{th}$ component of the input transmission matrix B.

The corresponding measurement or output of the state-space system is easily found by multiplying Eq. 84 by the measurement matrix C, that is,

$$\mathbf{y}_M(\tau) = C_M e^{\Lambda(\tau-\tau_0)}\mathbf{x}(\tau_0) + \int_{\tau_0}^{\tau} C_M e^{\Lambda(\tau-\alpha)} B_M\mathbf{u}(\alpha)d\alpha \tag{90}$$

which can also be expressed by applying the modal transformation as to obtain the m^{th}-component of the output y_m as

$$y_n(\tau) = \sum_{i=1}^{N_x} c_{ni}^T e^{\lambda_i(\tau-\tau_0)}\ x_i(\tau_0) + \sum_{i=1}^{N_x} \int_{\tau_0}^{\tau} c_{ni} e^{\lambda_i(\tau-\alpha)}\ b_{im} u_m(\alpha) d\alpha \text{ for } n = 1, \cdots, N_y \qquad (91)$$

with c_{ni} the $(n,i)^{th}$ component of the of output transmission matrix C. This is defined as the *modal representation* of the system [10].

It is also interesting to note that if we *constrain* this solution to be *only* homogeneous, then the response to the initial (condition) state vector is simply

$$\mathbf{x}_M(\tau) = e^{\Lambda(\tau-\tau_0)}\mathbf{x}_M(\tau_0)$$

or component-wise, we have

$$\mathbf{x}_i(\tau) = e^{\lambda_i(\tau-\tau_0)}\mathbf{x}_i(\tau_0) \qquad \text{for} \qquad i = 1, 2, \cdots, N_x \qquad (92)$$

where motion is expressed in terms of its eigenvalue–the natural frequency of the i^{th}-principal *mode* of vibration along with its corresponding eigenvector or *mode shape*.

Expanding this expression over i leads to the total solution or *modal decomposition* of the state-space as

$$\mathbf{x}_M(\tau) = e^{\Lambda(\tau-\tau_0)}\mathbf{x}_M(\tau_0) = \sum_{i=1}^{N_x} (\varepsilon_i e^{\lambda_i(\tau-\tau_0)}\eta_i^T)\mathbf{x}_i(\tau_0) \qquad \text{[Modal Decomposition]} \qquad (93)$$

that is, the homogeneous response is represented by a weighted superposition of system modes $\varepsilon_i e^{\lambda_i(\tau-\tau_0)}$ with the strength of each mode effected by $\mathbf{x}_i(\tau_0)$. Next we discuss the special case of distinct eigenvalues that are complex.

4.4 Complex Modes

With this in mind, we now extend the *modal state-space system* of the previous subsection to the complex modal case which is quite common in structural dynamics [4], [5]. For a typical structural system, the eigenvalues are complex, but still distinct. In this case the system matrix can be decomposed, as before, using the eigen-decomposition which now yields complex eigen-pairs along with the corresponding complex eigenvectors, that is,

$$\begin{aligned} \lambda_i &= -\sigma_i \pm j\omega_i \\ \\ \mathbf{t}_i &= [\xi_i \mid \xi_i^*] \quad \text{for} \quad i = 1, 2, \cdots, N_d \text{ for } N_x = 2 \times N_d \end{aligned} \qquad (94)$$

for N_d the dimension of the corresponding displacement vector of Eq. 5 and $\mathbf{t}_i$ the i^{th}-column vector of T_M with σ_i is the *damping coefficient*, ω_i the *damped natural frequency* and ϕ_i the *phase* such that

$$e^{-\sigma_i \tau} \times \cos\left(\omega_i \tau + \phi_i\right) \qquad \text{[Damped Sinusoid]}$$

Note that the *homogeneous* state and output responses are *real*, since

$$\mathbf{x}_M(\tau) = \sum_{i=1}^{N_x} 2e^{-\sigma_i(\tau-\tau_0)} \Re\{\mathbf{x}_i(\tau_0)\} = \sum_{i=1}^{N_x} 2e^{-\sigma_i(\tau-\tau_0)} |\mathbf{x}_i(\tau_0)| \cos\left(\omega_i \tau + \phi_i\right) \tag{95}$$

We also have that the modal transformation matrix becomes

$$T_M = \left[\xi_1 \; \xi_1^* \mid \xi_2 \; \xi_2^* \mid \cdots \mid \xi_{N_x/2} \; \xi_{N_x/2}^* \mid \right] \tag{96}$$

and applying this transformation to the system matrix A, we obtain

$$A_M = \Lambda = T_M \times A \times T_M^{-1} = \text{diag}\left(\left[\begin{array}{cc} \sigma_1 & \omega_1 \\ -\omega_1 & \sigma_1 \end{array} \right], \cdots, \left[\begin{array}{cc} \sigma_{N_x} & \omega_{N_x} \\ -\omega_{N_x} & \sigma_{N_x} \end{array} \right] \right) \tag{97}$$

with

$$B_M = T_M \times B; C_M = C \times T_M^{-1} \qquad \text{and} \qquad D_M = D$$

which leads to the modal state transition matrix for the complex eigen-system as

$$\Phi_M(\tau, \tau_0) = e^{\Lambda(\tau-\tau_0)} = \exp\left\{ \underbrace{\left[\begin{array}{ccc} \Lambda_1 & & 0 \\ & \ddots & \\ 0 & & \Lambda_{Nx} \end{array} \right]}_{\Lambda} (\tau - \tau_0) \right\} \text{ for } \Lambda_i = \left[\begin{array}{cc} \sigma_i & \omega_i \\ -\omega_i & \sigma_i \end{array} \right] \tag{98}$$

Thus, the complex modal state-space system is given by

$$\begin{aligned} \dot{\mathbf{x}}(\tau) &= A_M \mathbf{x}(\tau) + B_M \mathbf{u}(\tau) \\ \mathbf{y}(\tau) &= C_M \mathbf{x}(\tau) + D_M \mathbf{u}(\tau) \end{aligned} \tag{99}$$

where the system matrices become

$$A_M = \left[\begin{array}{cccc} A_{M_1} & 0 & \cdots & 0 \\ 0 & A_{M_2} & \cdots & 0 \\ \vdots & \vdots & \ddots & 0 \\ 0 & 0 & \cdots & A_{M_{N_x}} \end{array} \right]; B_M = \left[\begin{array}{c} B_{M_1} \\ \vdots \\ B_{M_{N_x}} \end{array} \right]; \; C_M = \left[C_{M_1} \mid \cdots \mid C_{M_{N_x}} \right]; \; D_M = D$$

and $A_{M_i} = \Lambda_i$.

This completes the MIMO *modal state-space description* that will be utilized in the model-based processor.

5 SPECTRAL ESTIMATION OF SIMULATED VIBRATION RESPONSE

In this section we study the application the various multichannel spectral estimators to extract modal frequencies of a vibrating structure represented by a *LTI*, *MIMO*, mass-spring-damper mechanical system consisting of 8-modes or 16-states (see [34] for details) measured by 3-output accelerometers. The structure is excited by a random input. Structurally, the system mass ($\mathcal{M}$) is characterized by an identity matrix while the coupled spring constants in (N/m) are given by the tri-diagonal matrix

$$\mathcal{K} = \begin{bmatrix} 2400 & -1600 & 0 & 0 & 0 & 0 & 0 & 0 \\ -1600 & 4000 & -2400 & 0 & 0 & 0 & 0 & 0 \\ 0 & -2400 & 5600 & -3200 & 0 & 0 & 0 & 0 \\ 0 & 0 & -3200 & 7200 & -4000 & 0 & 0 & 0 \\ 0 & 0 & 0 & -4000 & 8800 & -4800 & 0 & 0 \\ 0 & 0 & 0 & 0 & -4800 & 10400 & -5600 & 0 \\ 0 & 0 & 0 & 0 & 0 & -5600 & 12000 & -6400 \\ 0 & 0 & 0 & 0 & 0 & 0 & -6400 & 13600 \end{bmatrix}$$

the damping matrix is constructed using the relation (Raleigh damping)

$$\mathcal{C}_d = 0.680\mathcal{M} + 1.743 \times 10^{-4}\mathcal{K} \quad \left(\frac{N\ s}{m}\right)$$

The measurement system consisted of three (3) accelerometers placed to measure the modes at the 1, 4 and 8 locations on the structure. The accelerometer data is acquired and digitized at a sampling frequency of $50Hz$ ($\triangle t = 0.02sec$). The input signal from a randomly excited stinger rod is applied at a specified spatial location such that

$$\mathcal{M}\ddot{\mathbf{d}}(t) + \mathcal{C}_d\dot{\mathbf{d}}(t) + \mathcal{K}\mathbf{d}(t) = \mathcal{B}_p\mathbf{p}(t)$$

Three accelerometer outputs of the synthesized vibrating structure at a $0dB$ *SNR* were recorded for 200 *sec* with the vibrational responses shown in Fig. 1 along with their corresponding power spectra where we see a persistently excited system ideal for spectral estimation. The set of "true" modal frequencies corresponding to the spectral peaks are:

$$f_{TRUE} = \{2.94, 5.87, 8.60, 11.19, 13.78, 16.52, 19.54, 23.12 \quad Hz\}$$

The 3-accelerometer channels were processed by the multichannel classical spectral estimators: *BTM* and *WPM* with the output channel estimates shown in Fig. 2 and 3. Physically, some of the modes were *not* strongly excited at a given accelerometer location and therefore may not appear in the corresponding channel spectra. This implies that multichannel processing should provide superior performance in this case, since weak modes over

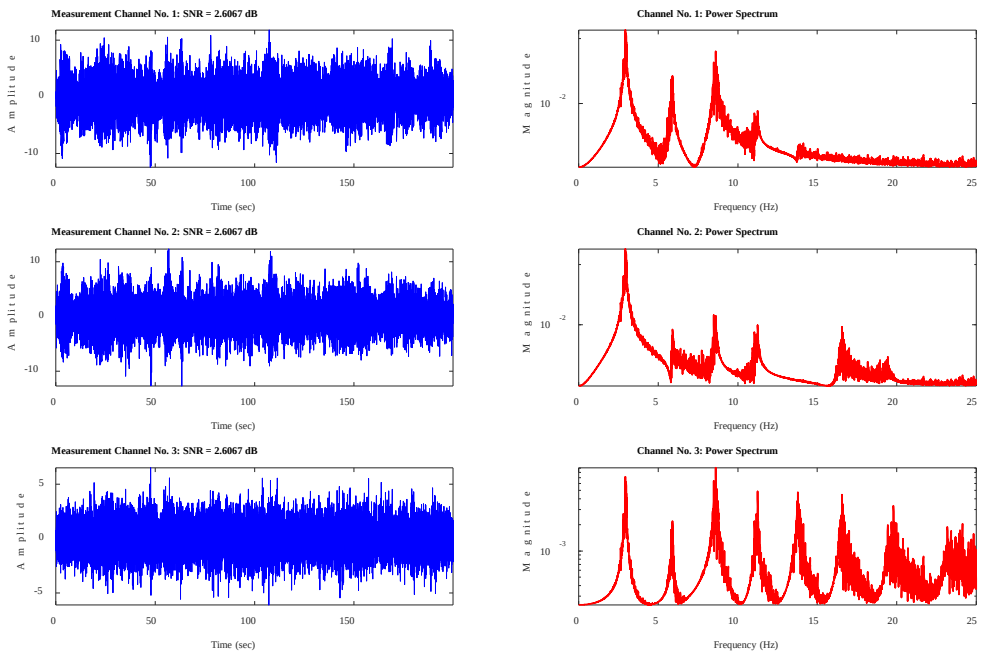

Figure 1: Structural vibrations of 8-mode mechanical system: (a) Accelerometer responses of 3-output system ($0db$ SNR). (b) Fourier power spectra of channel responses.

measurement channels accumulate their response and improve the signal levels. In any case the spectral estimates are shown in Fig. 2 and Fig. 3 for each technique. It is clear that the BTM has a much higher variance and the peaks are difficult to extract even though the power is present at the correct modal frequencies. The WPM estimate is much smoother than BTM (as expected), but its peak resolution is smeared decreasing spectral resolution. Four (4) of the 8 modal frequency peaks are clearly discernible. The classical multichannel methods are viable, but lack the high resolution capability of the parametric techniques to follow.

The multichannel Yule-Walker (YWM) spectral estimation results are shown in Fig. 4 with more of the spectral peaks extracted than the classical BTM and WPM methods. These modal peaks are primarily extracted because of its underlying 20^{th}-order multichannel autoregressive (all-pole) model embedded in the method. However, the peak estimates are somewhat inaccurate as summarized in Table 1 (with large outliers ignored and annotated by the asterisk). Next the high resolution family of multichannel Burg-lattice methods were applied to the synthesized structural data with more success as shown in Fig. 5 for the Morf-Viera method [21] and the Nutall method [22] of Fig. 6. Both 16^{th}-order, embedded, multichannel AR-models yield almost identical spectra (see the figures) as indicated by the

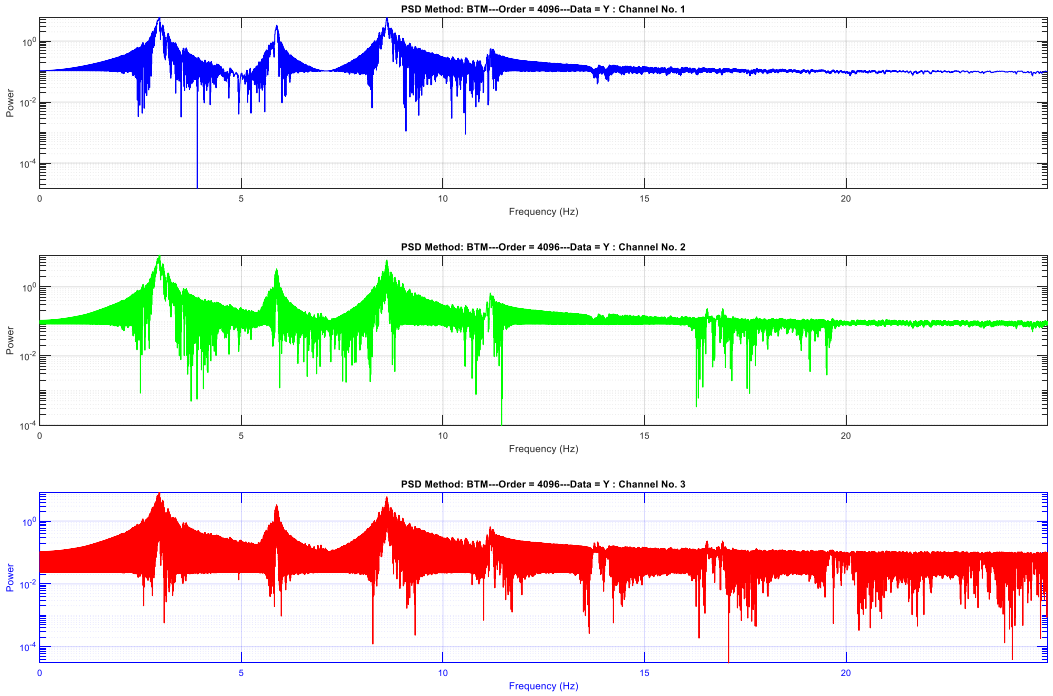

Figure 2: Multichannel Blackman-Tukey Method (BTM) Power Spectral Density Estimates for 8-mode, 3-channel structure.

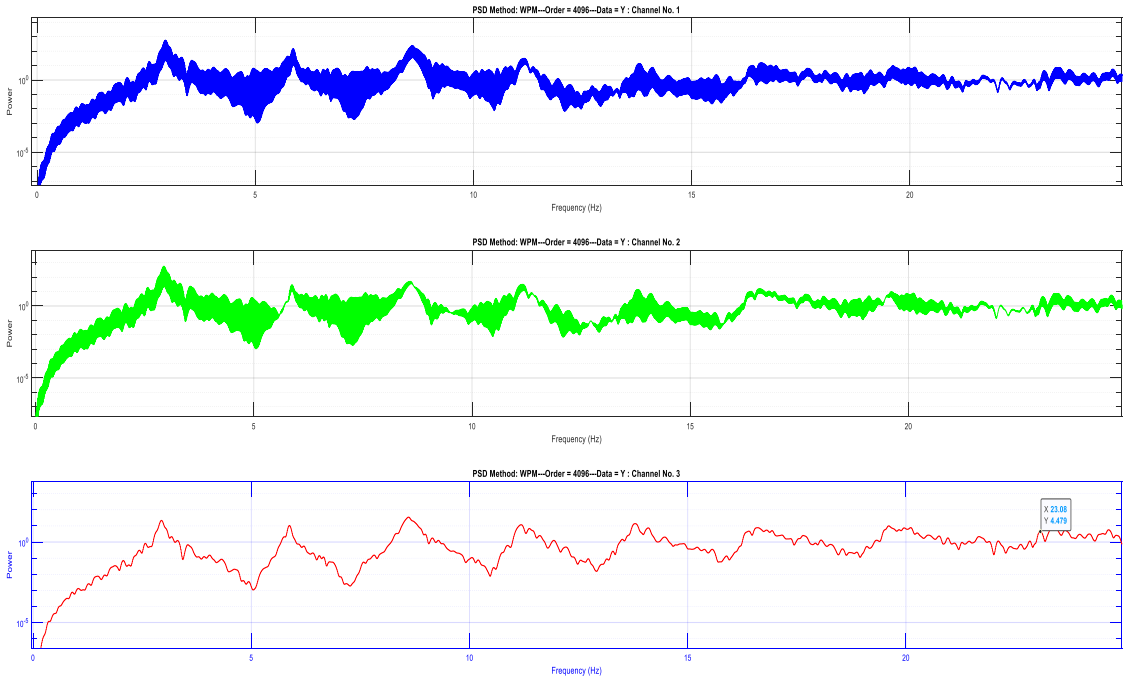

Figure 3: Multichannel Welch Periodogram Method (WPM) Power Spectral Density Estimates for 8-mode, 3-channel structure.

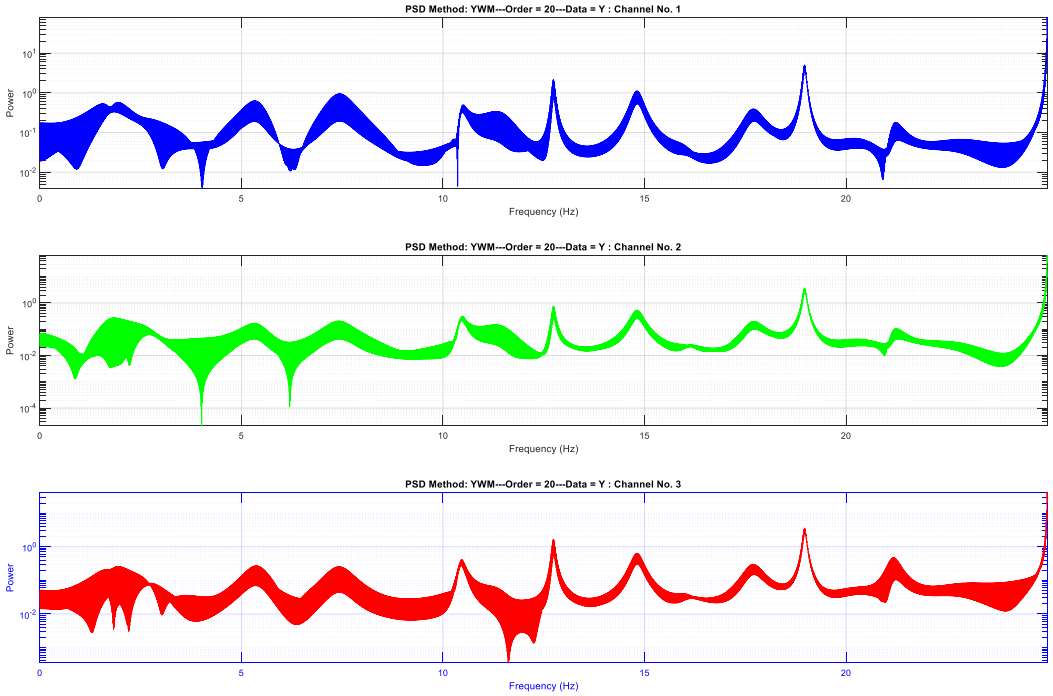

Figure 4: Multichannel Yule-Walker Method (YWM) Power Spectral Density Estimates for 8-mode, 3-channel structure.

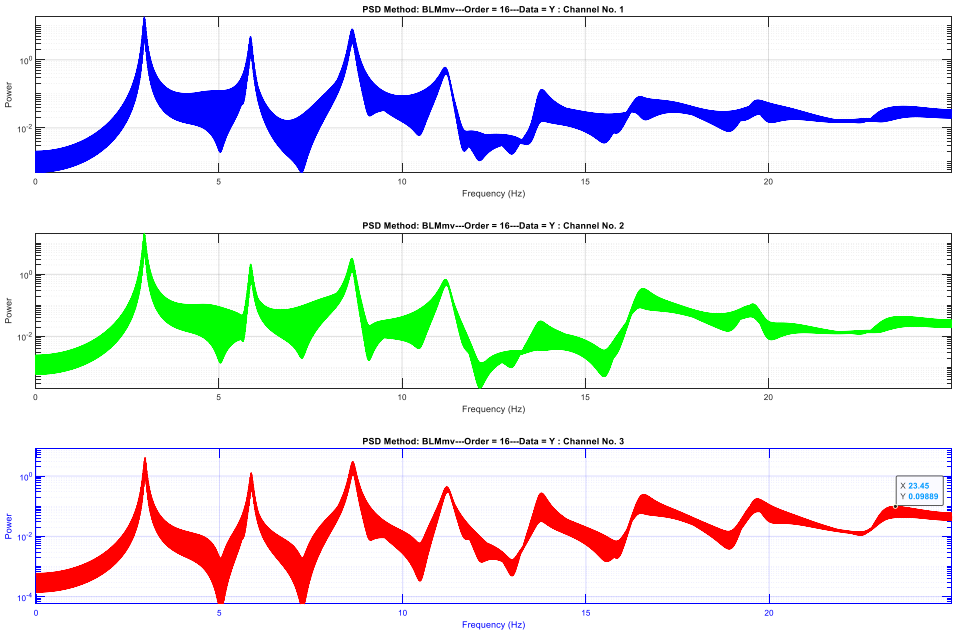

Figure 5: Burg Lattice Morf-Viera Method (BLMorfV) Power Spectral Density Estimates for 8-mode, 3-channel structure.

plots and results in Table 1. Next the multichannel minimum variance method (*MVM*) was applied to the data using a 20^{th}-order model assumption with the spectral (peak) estimates shown in Fig. 6 and Table 1. The *MVM* appears to perform similarly to the Burg-lattice methods as indicated by the modal frequency estimates.

Finally, we applied two model-based, state-space methods: $N4SID$ and its fast constrained counterpart. The **N**umerical method **4** **S**ubspace system **ID**entification (**N4SID**) is a *FULL* stochastic realization solution extracting the complete innovations model (Σ_{INV}) of the previous section, while the constrained method, based on the "output-only" method, is focused on exclusively estimating the process/output components $\{A, C\}$ of Σ_{INV}. Both methods employ projection theory and extract the modal eigen-frequencies from A and corresponding mode-shapes from C (see [26] for more details). Here the assumed excitation is the innovation or prediction error sequences, therefore, the estimated model admits a 3-input/3-output representation yielding 9 spectra composed of individual channel (diagonals) as well as cross-spectra (off-diagonals). The spectral estimation results for the *FULL* (stochastic realization) and *FAST* (constrained) model-based methods (*MBM*) are shown in Figs. 8 and 9 as well as the eigen-frequencies in Table 1 for comparison. Both methods yield close to identical modal frequencies; therefore, we only list one set of the *MBM* results. From the figures, it is interesting to observe the *MBM*s are able to extract the 8-modal frequencies on

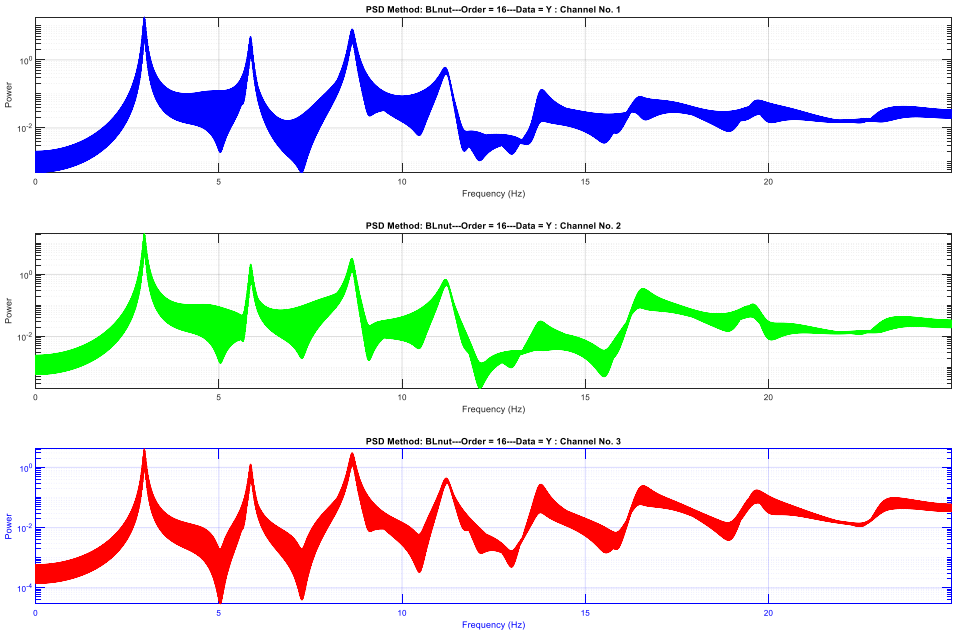

Figure 6: Burg Lattice Nutall-Strand Method (BLNutS) Power Spectral Density Estimates for 8-mode, 3-channel structure.

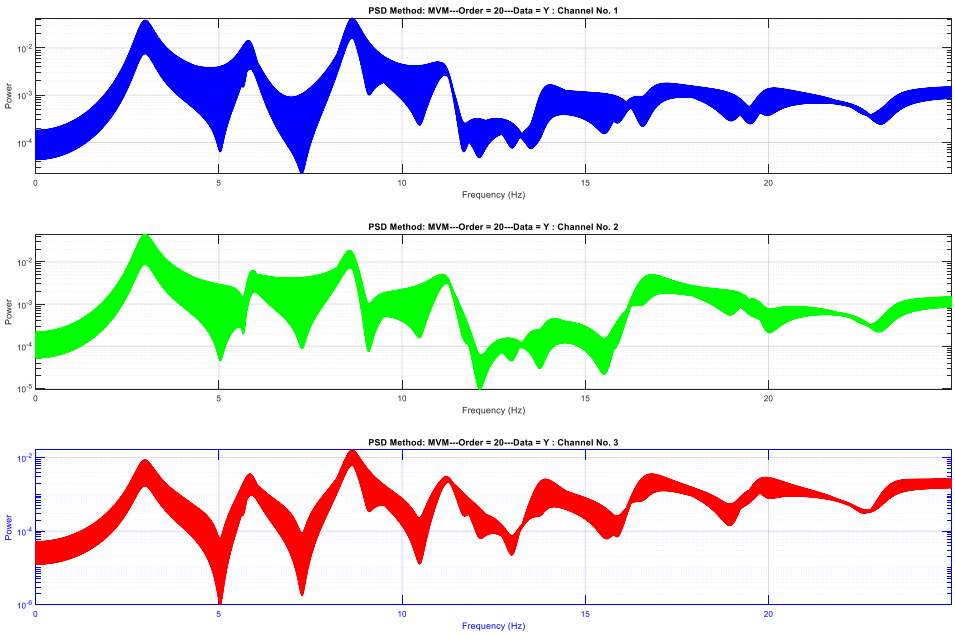

Figure 7: Minimum Variance Method (MVM) Power Spectral Density Estimates for 8-mode, 3-channel structure.

all of the channels as indicated by their corresponding spectra obtained by calculating the model (modal) impulse responses for each of the input-output pairs (channels). The results for the *FAST MBM* are shown in Fig. 9 illustrating the estimates channel/cross-channel impulse responses and the "average" spectrum. The strongest responses appear from the 3^{rd}-channels accelerometer measurements in which all-modes appear excited. Comparing the averaged the extracted modal frequencies for both the *FULL* and *FAST MBM*s in Fig. 10, we see that they are quite similar (see Table 1) and capture the essence of the modal responses implying that a potential real-time approach may be feasible.

Table 2.0 MULTICHANNEL SPECTRAL ESTIMATION (Channel) STATISTICS

MODAL Frequency Estimates (% Relative Error(ϵ))							
Frequency	BTM	WPM	YWM	BLMorfV	BLNutS	MVM	MBM
2.94 Hz	2.95(0.3)	2.95(0.3)	1.95(33.7)	2.97(1.0)	2.98(1.4)	2.98(1.4)	2.98(1.4)
—	2.91(1.0)	2.94(0.0)	2.94(0.0)	2.97(1.0)	3.00(2.0)	2.94(0.0)	2.98(1.4)
—	2.95(0.3)	2.94(0.0)	2.94(0.0)	2.94(0.0)	2.97(1.0)	2.98(1.4)	2.93(0.3)
5.87 Hz	5.90(0.5)	5.87(0.0)	5.33(9.2)	5.85(0.3)	5.87(0.0)	5.80(1.2)	5.91(0.7)
—	5.90(0.5)	5.86(0.2)	5.86(0.2)	5.88(0.2)	5.82(0.9)	5.86(0.2)	5.91(0.7)
—	5.86(0.2)	5.90(0.5)	5.90(0.5)	5.87(0.0)	5.87(0.0)	5.85(0.3)	5.36(8.7)
8.60 Hz	8.59(0.1)	8.59(0.1)	7.43(13.5)	8.66(0.7)	8.63(0.4)	8.57(0.4)	8.60(0.0)
—	8.60(0.0)	8.60(0.0)	8.60(0.0)	8.63(0.4)	8.60(0.0)	8.60(0.0)	8.65(0.6)
—	8.57(0.4)	8.59(0.1)	8.59(0.1)	8.64(0.5)	8.64(0.5)	8.63(0.4)	8.60(0.0)
11.19 Hz	11.15(0.4)	11.17(0.3)	11.34(1.3)	11.16(0.3)	11.16(0.3)	11.09(0.9)	11.29(0.9)
—	11.15(0.4)	11.15(0.4)	11.15(0.4)	11.16(0.3)	11.11(0.8)	11.15(0.4)	11.34(1.3)
—	11.19(0.0)	11.19(0.0)	11.19(0.0)	11.20(0.9)	11.21(0.2)	11.19(0.0)	11.19(0.0)
13.78 Hz	13.79(0.1)	13.80(0.2)	14.82(7.6)	13.79(0.1)	13.80(0.2)	13.99(0.0)	13.88(0.0)
—	13.79(0.1)	13.80(0.2)	13.80(0.2)	13.78(0.0)	13.75(0.2)	14.16(2.8)	13.98(1.5)
—	13.81(0.2)	13.79(0.1)	13.79(0.1)	13.79(0.1)	13.79(0.1)	13.91(0.9)	13.78(0.0)
16.52 Hz	16.61(0.6)	16.58(0.4)	16.58(0.4)	16.51(0.1)	16.48(0.2)	17.08(3.4)	16.76(1.5)
—	16.56(0.2)	16.58(0.4)	16.58(0.4)	16.56(0.2)	16.56(0.2)	16.76(1.5)	16.62(0.6)
—	16.57(0.3)	16.60(0.5)	16.60(0.5)	16.59(0.4)	16.58(0.4)	16.81(1.8)	16.57(0.3)
19.54 Hz	19.59(0.3)	19.61(0.4)	19.61(0.4)	19.75(1.1)	19.69(0.8)	19.99(2.3)	19.89(1.8)
—	19.59(0.3)	19.61(0.4)	19.61(0.4)	19.54(0.0)	19.61(0.4)	19.18(0.0)	19.89(1.8)
—	19.61(0.4)	19.61(0.4)	19.61(0.4)	19.67(0.7)	19.67(0.7)	19.89(1.8)	19.65(0.6)
23.12 Hz	23.07(0.2)	23.08(0.2)	23.08(0.2)	23.49(1.6)	23.45(1.4)	23.76(2.8)	23.61(2.1)
—	23.08(0.2)	23.08(0.2)	23.08(0.2)	23.46(1.5)	23.42(1.3)	23.82(3.0)	23.56(1.9)
—	23.06(0.3)	23.08(0.2)	23.08(0.2)	23.45(1.5)	23.34(1.0)	23.48(1.6)	23.17(0.2)
Avg (%ϵ)	(0.30%)	(0.26%)	(0.35%*)	(0.54%)	(0.60%)	(1.19%)	(0.86%)

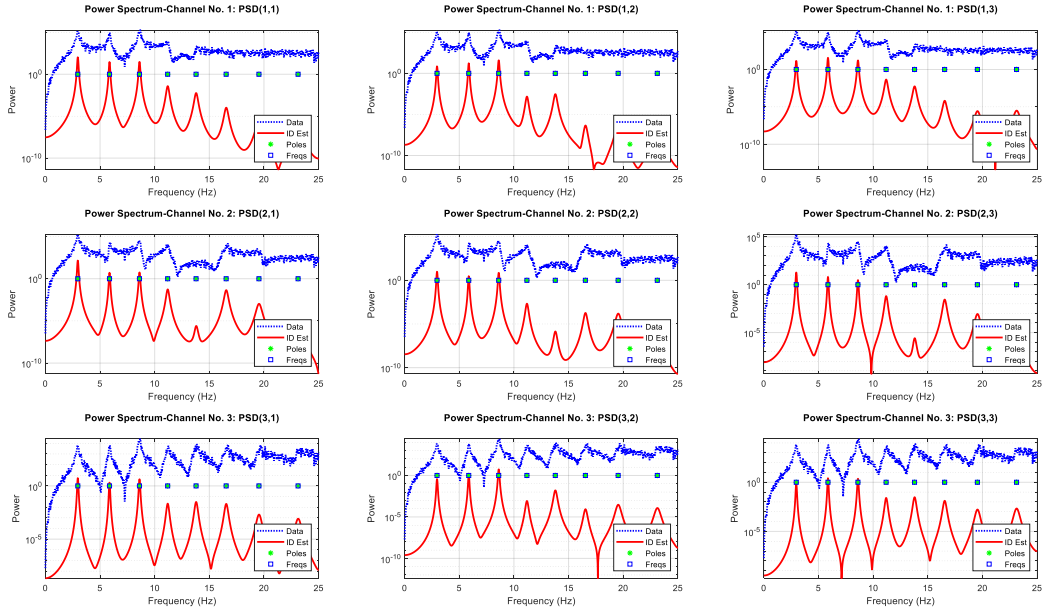

Figure 8: FULL (stochastic realization) Model-Based Method (N4SID) Power Spectral Density Estimates for 8-mode, 3-channel structure.

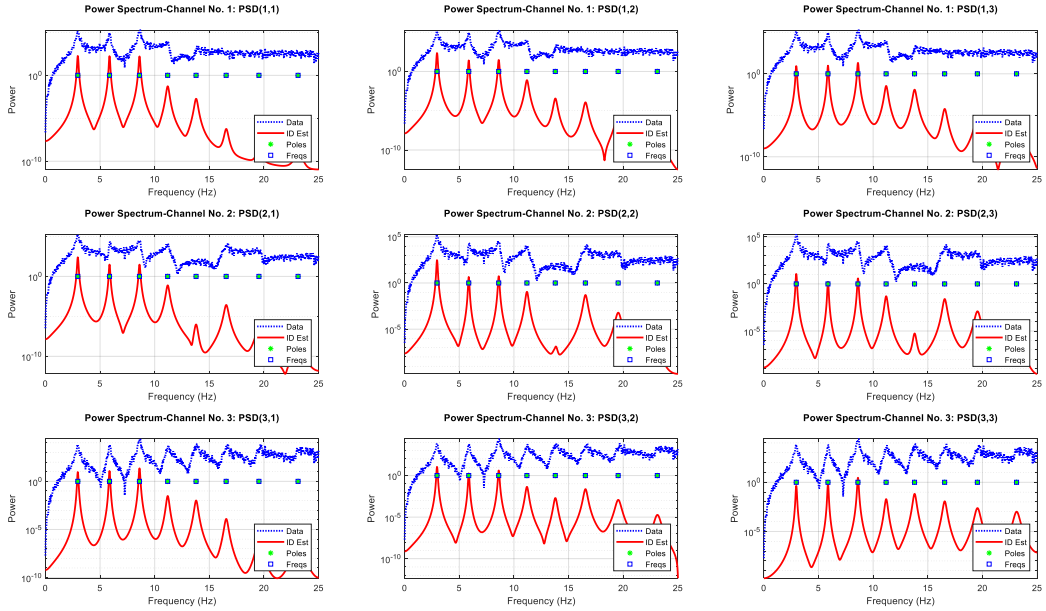

Figure 9: FAST Model-Based (Constrained) Method Power Spectral Density Estimates for 8-mode, 3-channel structure.

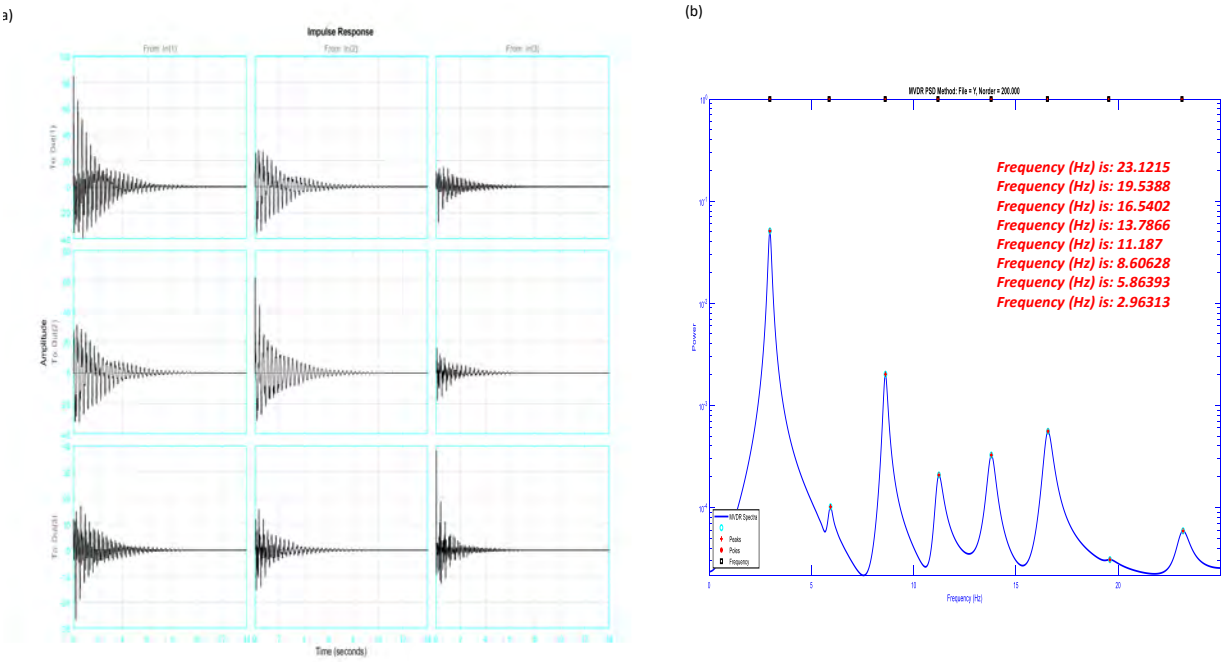

Figure 10: FAST Model-Based Method (N4SID) Estimates for 8-mode, 3-channel structure. (a) Impulse response (modal) estimates. (b) Average spectral estimate (modal frequencies).

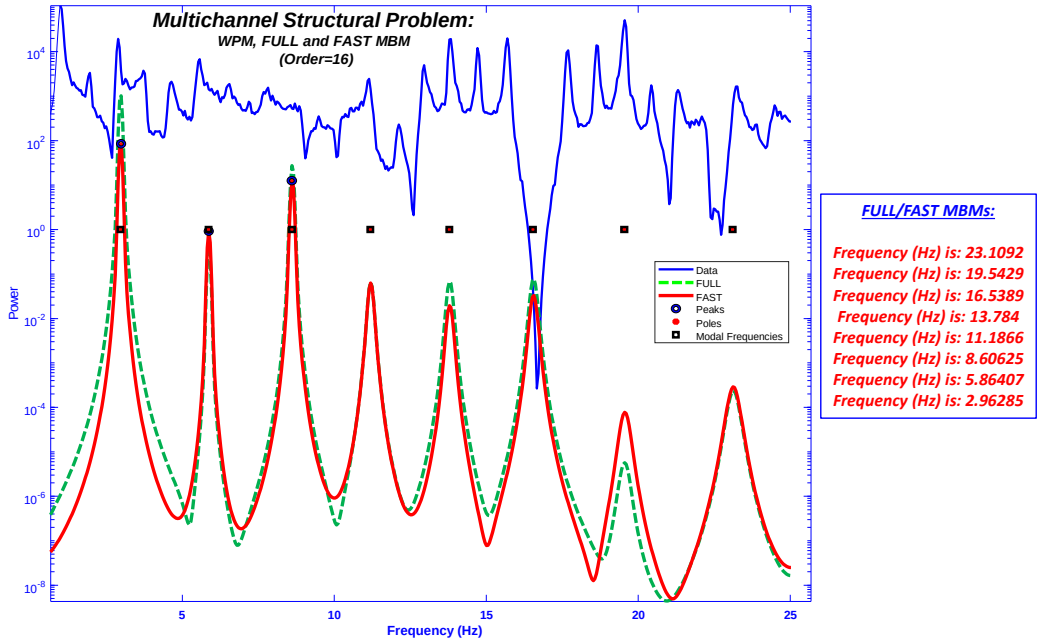

Figure 11: COMPARISON FULL/FAST Model-Based Method (*MBM*) Estimates for 8-mode, 3-channel structure: Average Power Spectra with Average modal frequency estimates.

6 SUMMARY

In this report we have investigated the performance of "classical" multichannel spectral estimation techniques. We chose the two most popular and well-known techniques: Blackman-Tukey method (*BTM*) and Welch Periodogram (average) method (*WPM*). Along with these methods, we investigated a suite of "modern" parametric estimators based on the multichannel autoregressive model as well as the model-based state-space representation. The classical and *AR*-models provided reasonable estimates for the $0dB$ SNR test case evolving from a synthesized 8-mode, 3-output, structural system that was developed to evaluate the performance of each method. From the respective multichannel estimates, the classical as well as the modern methods produces noisy spectra while the corresponding model-based approaches were much smoother with very well defined modal frequences. It was surprising that the calculated relative errors of Table 1 did not reflect the superiority of the *MBM* although all of these errors were $< 2\%$ indicating a set of reasonable results. Note that the corresponding frequencies were all determined by visual peak-picking that created some of the uncertainty especially when the spectral peaks were not well-defined. The *MBM*, however, obtain the modal frequency estimates directly from the corresponding embedded state-space models probably indicating a more realistic set of relative frequency errors. The final conclusion is that the classical, modern and model-based methods can be used to provide reasonable multichannel spectral estimates, but that real-time implementation still poses a great challenge.

7 Acknowledgments

This work performed under the auspices of the U.S. Department of Energy by Lawrence Livermore National Laboratory under Contract DE-AC52-07NA27344.

References

[1] P. Welch, "The use of fast Fourier transforms for the estimation of power spectra: A method based on time averaging over short modified periodograms," *IEEE Trans. Audio Electroacoust.*, AU-15, 1967.

[2] J. Candy, S. Franco, E. Ruggiero, M. Emmons, I. Lopez and L. Stoops, "Anomaly detection for a vibrating structure: A subspace identification/tracking approach, *J. Acoust. Soc. Am.*, Vol. 142, (2), pp. 680-696, 2017.

[3] M. Junger and D. Feit, *Sound: Structures and Their Interaction*. $2^{Ed.}$ Cambridge, MA: MIT Press, , 1986.

[4] M. R. Hatch, *Vibration Simulation Using MATLAB and ANSYS*. Boca Raton,FL.:Chapman and Hall/CRC Press, 2001.

[5] W. K. Gawronski, *Advanced Structural Dynamics and Active Control of Structures*. London, U.K.:Springer, 2004.

[6] C. Rainieri and G. Fabbrocino, *Operational Modal Analysis of Civil Engineering Structures*. London,U.K.:Springer, 2014.

[7] L. Merovitch, *Analytic Methods in Vibrations*. New York: MacMillan Pubs, 1996.

[8] J. Cooley and J. Tukey, "An algorithm for machine calculation of complex Fourier series," *Math. Comput.*, 1965.

[9] S. Kay, *Modern Spectral Estimation: Theory and Applications*, Englewood Cliffs, New Jersey:Prentice-Hall, 1988.

[10] T. Kailath, *Linear Systems*, Upper Saddle River, N.J.:Prentice-Hall, 1980.

[11] R. A. DeCarlo, *Linear Systems: A State Variable Approach with Numerical Implementation*, Engelwood Cliffs, N.J.:Prentice Prentice Hall, 1989.

[12] A. Schuster, "On the Investigation of Hidden Periodicities with Application to a Supposed 26 Day Period of Meteorological Phenomena," *Terrestrial Magnetism*, Vol. 3, 1898.

[13] P. Stoica and R. Moses, *Introduction to Spectral Estimation*, Englewood Cliffs, New Jersey:Prentice-Hall, 1997.

[14] J. Markel and A. Gray, *Linear Prediction of Speech*, New York:Springer-Verlag, 1976.

[15] J. Candy, *Signal Processing: The Modern Approach* (New York:McGraw-Hill, 1988).

[16] S. Kay and L. Marple, "Spectrum analysis – a modern perspective," *Proc. IEEE*, Vol. 69, 1981.

[17] D. Childers, Ed., *Modern Spectral Analysis*, New York:IEEE Press, 1978.

[18] L. Marple, *Digital Spectral Analysis*,2nd Ed., Mineola, New York:Dover Pubs., 2019.

[19] E. Robinson and S. Treitel, *Geophysical Signal Analysis* (New Jersey:Prentice-Hall, 1980).

[20] J. Burg, *Maximum Entropy Spectral Analysis*, PhD Dissertation, Palo Alto, CA:Stanford Univ., 1975.

[21] M. Morf, A. Viera, D. Lee, and T. Kailath, "Recursive multichannel maximum entropy spectral estimation," *IEEE Trans. Geosci. Electron.*, Vol. GE-16, pp. 85-94, 1978.

[22] A. Nutall, *Multivariate linear predictive analysis employing weighted forward and backward averaging*, **NUSC Report**, No. 5501, New London, Conn., 1976.

[23] L. Ljung, *System Identification: Theory for the User*.2e Englewood Cliffs, N.J.:Prentice-Hall, 1999.

[24] J. Candy, *Model-Based Signal Processing*, Hoboken, New Jersey: John Wiley/IEEE Press, 2006.

[25] B. Ho and R. Kalman, "Effective reconstruction of linear state variable models from input/output data," Regelungstechnik, 14, , 545-548, 1966.

[26] J. Candy, *Model-Based Processing: An Applied Subspace Identification Approach*, (Hoboken,N.J.: John Wiley, 2019), 511 pages.

[27] H. Akaike, "Stochastic theory of minimal realization," *IEEE Trans. Auto. Contr.*, 19, pp. 667-674, 1974.

[28] M. Aoki, *State Space Modeling of Time Series*, 2nd Ed. (London, U.K.: Springer-Verlag, 1990).

[29] P. van Overschee and B. De Moor, *Subspace Identification for Linear Systems: Theory, Implementation, Applications* (Boston, MA: Kluwer Academic Publishers, 1996).

[30] T. Katayama, Subspace Methods for System Identification. (London, U.K.: Springer, 2005).

[31] E. Reynders, "System identification methods for (operational) modal analysis: review and comparison," *Archiv. Comput. Methods Engr.*, Vol. 19, No. 1, pp. 51-124, 2012.

[32] J. Juang, Applied System Identification. Upper Saddle River, N.J.: Prentice-Hall PTR, 1994.

[33] H. Zeiger and A. McEwen, "Approximate linear realization of given dimension via Ho's algorithm," IEEE Trans. Automat. Contr., vol. AC-19, no. 2, pp. 153, 1974.

[34] F. Cara, J. Juan, E. Alarco, E. Reynders, G. De Roeck, "Modal contribution and statespace order selection in operational modal analysis," *Mech. Sys. Sig. Process.*, Vol. 38, 2013.

[35] A. Papoulis, *Probability, Random Variables and Stochastic Processes* (New York:McGraw-Hill, 1965).

[36] A. Jazwinski, *Stochastic Processes and Filtering Theory*, New York:Academic Press, 1970.